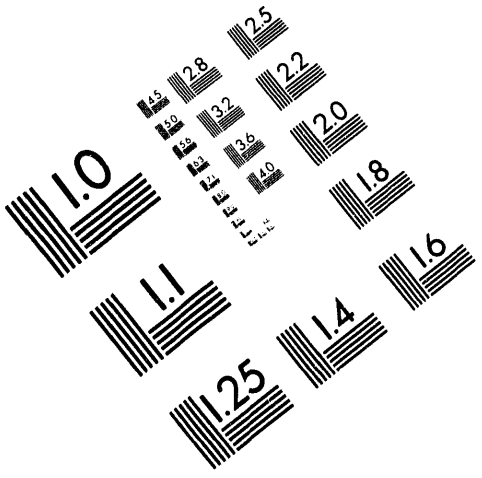

Association for Information and Image Management

1100 Wayne Avenue, Suite 1100
Silver Spring, Maryland 20910

301/587-8202

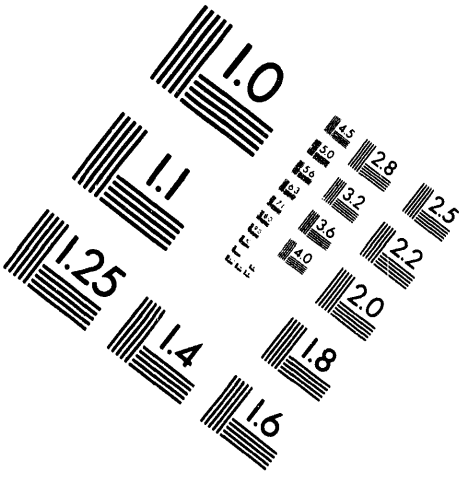

Centimeter

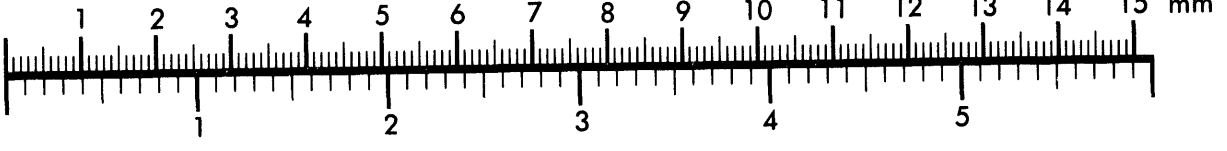

Inches

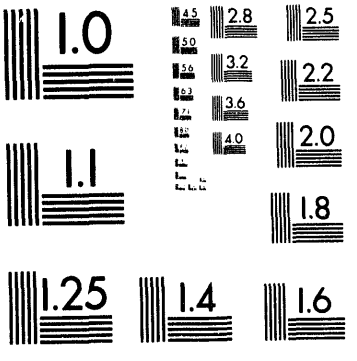

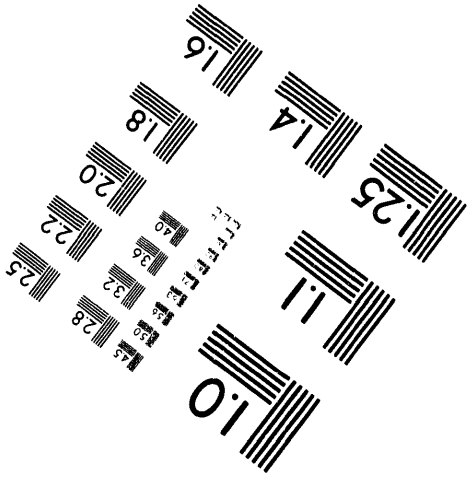

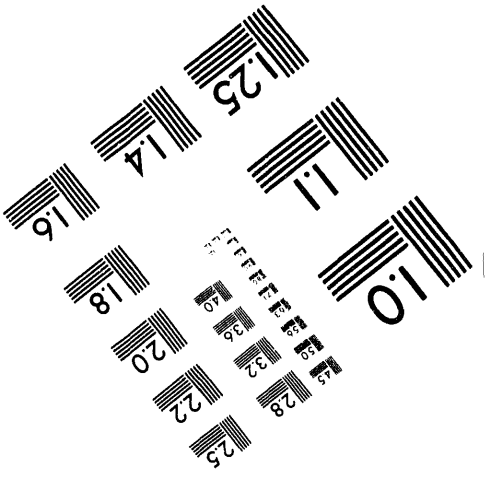

MANUFACTURED TO AIIM STANDARDS
BY APPLIED IMAGE, INC.

1 of 1

High power phase conjugated solid state lasers

L. A. Hackel, C. B. Dane, L. E. Zapata, and M. R. Hermann

Lawrence Livermore National Laboratory
Livermore, CA 94550

Abstract

Three laser systems that are being developed for use in x-ray generation which incorporate SBS phase conjugate mirrors are described. A 25 J/pulse Nd:glass laser is being developed for commercial proximity print x-ray lithography; a 0.5 J/pulse, 1.3 kHz pulse repetition frequency laser is being built for soft x-ray projection lithography; and a 1 kJ/pulse laser driver for a table top x-ray laser has been designed. The results of prototypical experimental investigations are presented and the basic design principles for high average power phase conjugated laser systems shared by each of these lasers are discussed.

I. Introduction

Over the last 20 years lasers have become an increasingly useful tool for the generation of x-ray radiation. In particular, recent technological advances have allowed solid state lasers to be designed for use in the near term as drive sources for proximity print x-ray lithography systems as well as in the longer term for soft x-ray projection lithography systems.[1,2] In addition advances in laser technology allow the building of multi-hundred joule per pulse, several nanosecond pulse length lasers with moderate average power and table top size. This development now enables the design of table top x-ray sources and x-ray lasers with important uses in medicine and biology.

Within our laboratory we have been developing high power solid state lasers as drivers for producing the x-rays required for these systems. Nonlinear optics is playing an important role in the design of each of these laser systems, from the generation of high beam quality, to the stage to stage gain isolation, to the compression of high power pulses. A particularly important aspect for almost every system we have developed is the use of phase conjugate mirrors. These mirrors function in two important respects: they provide a means to obtain very high beam brightness without the generation of hot spots which damage optical components and because of their threshold activation characteristic they function in the role of multistage gain isolators.

In this paper we briefly describe three specific lasers we are building for use in x-ray systems: first, the design and performance of a multi-joule Nd:glass laser which is being

MASTER

hardened for commercial proximity print x-ray lithography, second, a half joule per pulse, 1.3 kHz repetition rate laser which is being built for projection lithography and third, a system which is in the design phase and will be used as a pump source for an x-ray laser.

II. 25 J/pulse Nd:glass laser for proximity print lithography

A. Lithography considerations

Proximity print x-ray lithography is at the forefront of efforts to develop a commercial lithography system capable of producing circuit feature of 0.35 μm and smaller. A schematic of the concept is shown in Figure 1 where a 20 J/pulse, 10 to 20 ns pulse length laser output is focused to a ~200 μm diameter spot at a metal or dense gas target. For example, when using an iron target, the pulse creates and heats a plasma generating x-ray emission in the range of 10 to 15 Å. At a 20 to 40 cm distance the x-rays generated from this "point source" target pass through a mask which is placed several microns above a resist coated silicon wafer. The mask contains a replica of the circuit features to be printed allowing x-rays to pass through a transparent areas and activate the exposed resist. The process is repeated on approximately 80 of such fields on a typical six inch wafer followed by a development, etching and washing process to create the circuit features. For the rapid printing required in a commercial process this technique has required advances in scanner capability to rapidly move and precisely align to each succeeding field as well as the development of a source capable of providing 10 mJ/cm2 of x-ray flux over time periods of several seconds. This requirement translates into an ultimate laser power requirement for a full production quality machine of approximately 500 W to 1 kW with a focused power density of 10^{13} to 10^{14} W/cm^2.

B. Laser design

We have developed a laser system capable of performing the proximity print lithography task. The system employs an Nd:glass laser using regenerative amplifier technology and produces near diffraction limited output beams with 25 joules per pulse and up to a 5 Hz pulse repetition rate. A simple modification to the laser allows the addition of a second amplifier head which operates for 50% of the duty cycle and thus allows effective repetition rates of 10 Hz. Our initial development version of this laser was described at the first International School on Nonlinear Optics.[3] However the present upgraded system which we present here is simpler, more robust in high energy output, and operates at a higher average power.

The basic design of the laser is shown in Figure 2. In this design, the output of a master oscillator is tailored to the desired pulse length, beam quality, and repetition rate and is then amplified to the desired energy in an eight pass regenerative amplifier. The low power master oscillator is operated in a self seeded mode to produce single frequency, diffraction limited output. The oscillator output is preamplified, anamorphically expanded, and then imaged into the regenerative amplifier ring. The ring amplifier is configured with a polarizer and 90° polarization rotator which act as a passive

polarization switch. The input beam transits the ring once, double passing the Nd:glass amplifier (small signal amplification of ~3/pass), rotates in polarization and passes the ring a second time (obtaining 4 total gain passes at this point). After the second ring pass the polarization has rotated to deflect the beam to the phase conjugate mirror. The energy delivered to the conjugate mirror is ~2.5 J.

Details of this laser system have previously been described.[4] For x-ray lithography, the oscillator output is amplified to approximately 25 J/pulse in a 14 ns pulse length. However the laser design can also be adapted for pulse lengths of up to 500ns. By using a longer master oscillator pulse, making specific changes to the phase conjugate mirror, and substituting a Faraday rotator for the input/output Pockels cell, the laser can be run in a long pulse (~500ns) mode. This opens up additional applications where long, coherent pulse lengths are desirable.

The regenerative amplifier optical configuration is ideally suited to solid state gain media such as Nd:glass. The small stimulated emission cross section (3.5×10^{-20} cm^2) and long spontaneous lifetime (350 μs) of phosphate glasses give this medium good energy storage characteristics and permit an amplifier system to be operated with many passes and a large system gain without significant losses to amplified spontaneous emission (ASE). The regenerative amplifier effectively provides these gain passes without the complicated optical staging of more conventional master oscillator power amplifier (MOPA) configurations in which extraction beams are angularly multiplexed through amplifier sub-apertures of increasing size.

Optimal extraction efficiency from a zig-zag slab gain medium requires the amplification of a near top hat spatial beam profile. However, the high aspect ratio rectangular slab aperture combined with this spatial profile results in a beam with poor near field propagation characteristics, particularly in the presence of thermally induced phase aberrations in the solid state amplifier. For this reason, our design uses a 1:1 relay imaging telescope inside of the regenerative amplifier ring which re-images each plane inside the zig-zag slab back onto itself, preserving uniform irradiance spatial profiles in the amplifier for multiple ring passes. A significant part of the design of this system is the use of a double-pass relay telescope as illustrated in Figure 2. The telescope consists simply of two lenses mounted with an afocal spacing as pressure windows on a vacuum chamber. The counter-propagating beams pass through the lenses offset from the optical axis allowing two separate optical paths through the telescope.

The double-pass telescope geometry offers a number of advantages over a single-pass design. First, it allows the telescope to be constructed with two refractive optics without folding the internal beam paths with reflective mirrors. With only a single pass through a simple two lens telescope, the distance between the conjugate planes would be insufficient to close the regenerative amplifier ring. A more complex multi-element folded relay telescope could be used to extend the distance between the conjugate planes. However, this would require that a number of optical surfaces be located at effectively large propagation distances from the image plane in the laser amplifier. In this case, amplitude modulation due to the propagation of diffraction at the edge of the

top hat beam and the propagation of thermal aberrations introduced in the amplifier significantly increases the possibility of damage to optics far from this optical relay plane. A second important advantage of the double passed relay telescope is that it provides an external relay plane on the output of the laser system in which, for example, a frequency doubler can be placed. The same smooth irradiance spatial profile present in the zig-zag slab is relayed into the doubler resulting in uniform second harmonic generation across the output aperture.

The goal of the amplifier head design is to maximize the efficiency and uniformity of the upper laser level activation in the gain medium while minimizing thermally induced distortion and depolarization of the transmitted optical wavefront. The major components of the amplifier design are the zig-zag slab, the cooling system, and the flashlamp and reflector assemblies.

The choice of a slab geometry requires analyses of the gain and energy storage required for the desired output energy, the ASE energy storage losses, and the thermally induced optical aberration and depolarization. The amplifier slab design for this regenerative amplifier system is illustrated in Figure 3. The zig-zag slab is 1 cm wide, 14 cm tall, and 40 cm long for a total volume of 0.56 ℓ. It is composed of the neodymium (Nd) doped phosphate glass APG1 supplied by Schott Glass Technologies Inc. or HAP4 supplied by Hoya Corporation. The Nd doping level in both cases is 3×10^{20} cm^{-3} or 2.7% by weight. The laser beam enters the slab ~13° from the long slab axis so that it is reflected three times from each side of the slab, for a total of six bounces, before exiting the other end. This pathway, combined with the counter-propagating second path, provides nearly 100% optical fill and forms a six diamond pattern through the amplifier.

To minimize the possibility of internal parasitic oscillation, 2 mm thick copper doped absorbing glass is attached to the top and bottom edges of the glass amplifier slab using an index of refraction matching elastomer, as illustrated in Figure 3. In addition, the input and output faces are parallel, but oriented 1.5° from normal so that a ray perpendicular to one face cannot intersect the opposite face. Numerical modeling indicates that a larger wedge angle on the slab end faces could further decrease stored energy losses due to ASE and allow an even higher maximum gain coefficient to be achieved. However, the use of indexed matched edge cladding with this near square ended slab geometry easily results in the required stored energy to efficiently extract a 25 J laser pulse.

C. *The phase conjugate mirror*

Our phase conjugate mirror employs stimulated Brillouin scattering (SBS). The basic concept of SBS phase conjugation is well understood and widely documented in the literature. However, there are a number of important considerations to be made when incorporating an SBS phase conjugate mirror into a high power laser system in order to accommodate the often required high input energies and to maintain good near and far field fidelity in the output.

For this application we use a two cell arrangement configured as an oscillator and amplifier. The cells are filled with a material possessing electrostrictive properties, for example, CCl_4. The light enters the first (amplifier) cell at a nominal size and is then focused using an approximately F/10 lens into the second (oscillator) cell This combination comprises the SBS phase conjugate mirror.

In addition to improving beam quality, there are additional significant advantages to the operation of the amplifier system with the SBS phase conjugator. Eight gain passes through the zig-zag slab amplifier can be achieved using passive polarization switching in the regenerative amplifier ring. The fact that the SBS cell provides interstage gain isolation makes this possible since, if it were replaced with a mirror, the small signal gain through eight consecutive gain passes would result in possible parasitic oscillation from the small reflective losses of AR coated optical surfaces in the ring or in the output beam. When the Pockels cell is located inside the regenerative amplifier ring, the length of the laser pulse to be amplified is limited to the transit time inside the ring minus the high voltage switching time for the Pockels cell. Now, with passive polarization switching, this time limit is increased to be the transit time for four ring revolutions. Longer pulses can be amplified and the relative timing accuracy requirement between the injected pulse and the Pockels cell voltage pulse is greatly reduced. In fact, the replacement of the Pockels cell with a full aperture Faraday isolator has been shown to allow the amplification of laser pulses of up to 500 ns in duration.[5]

The SBS phase conjugator very effectively conjugates the first order aberration of tilt. This greatly reduces the sensitivity of the system performance to small changes of optical alignment in the ring. No change in output power or pointing direction during operation are observed for large mirror misalignments in the ring, limited only to those angular excursions that result in vignetting of the beams at the edges of the amplifier slab.

1. Wavefront reversal fidelity

It has been proposed that for optimal wavefront reversal fidelity, the SBS phase conjugator should not be operated more than five times above the threshold of stimulated Brillouin return.[6] In that report, large shot to shot fluctuations in the wavefront of the Stokes output were measured when the SBS threshold was greatly exceeded. However, we have recently demonstrated that this observation was related to the slope of the rising edge of the input laser pulse relative to the acoustic decay time (τ_B) in the Brillouin medium.[7] It was shown that the results of Ref. 6 could be reproduced by placing a very fast leading edge on the input pulse. Of more importance, however, it was also shown that these fluctuations could be reduced by tailoring the rise time of the leading edge of the pulse such that it was longer than τ_B for the SBS material. Using carbon tetrachloride (CCl_4) with τ_B~1 ns and 13 ns FWHM input pulses with near Gaussian temporal profiles, good shot to shot fidelity was demonstrated at over 100 times above threshold. Based on these measurements, CCl_4 was chosen as the SBS medium for this amplifier system.

The conclusion that good wavefront reversal fidelity in the SBS Stokes waves is obtainable for input powers high above threshold is very significant given that there are strong motivations for operating the SBS phase conjugator with large input energies. Figure 4 schematically illustrates a simplified understanding of the SBS phase conjugation process. An input wave with a uniform irradiance spatial profile and flat phase profile is transmitted through an aberrating medium. If this beam is then focused into an SBS cell, the aberrated wavefront is transformed into a distorted irradiance spatial profile in the far field. The Stokes wave is seeded from random acoustic fluctuations in the medium and is selectively amplified by stimulated scattering in the regions of peak irradiance. The diffraction of the resulting counter propagating wave then produces a reversed, or phase conjugated, wavefront at the focusing lens. Based on this description, albeit a simple one, it can be reasoned that it is desirable to operate far above threshold with a highly aberrated input beam in order for the highest frequency modes, which often appear as small side lobe structures, to reach threshold and be reversed.

2. SBS amplifier / oscillator configuration

In general, the limit to the peak power that can be delivered to a focused SBS phase conjugate mirror is determined by competing processes such as stimulated Raman scattering, self focusing, and optical breakdown. This limitation can be overcome by using a two cell system configured in an oscillator / amplifier arrangement.[8] As depicted in the optical layout of Figure 2, the collimated input beam is directed through the first SBS cell and then focused into a second cell. In this way the peak optical power in the focused oscillator cell is reduced by the SBS amplification of the Stokes wave in the collimated amplifier cell. The beam cross section in the collimated cell is nominally adjusted such that the peak gain, irradiance, and length product (gIL) is ~30, near the threshold for stimulated return from that cell alone. In practice, however, it is found that very efficient amplification in the first cell is achieved with a calculated peak gIL product of ~45. Even at this large value, no spontaneous SBS contribution is observed from the amplifier cell since saturation of the incoming laser pump pulse prevents the gain product from reaching the estimated value.

Another consideration in configuring the SBS oscillator/ amplifier system is the round trip optical propagation length in the SBS medium. This should not greatly exceed τ_B for the SBS material. In this case, when the SBS system is driven high above threshold, strong pulse reshaping in the Stokes return in the form of pulse compression can result. For input pulses of sufficient duration, periodic modulation with a period corresponding to the round trip time through the SBS cells is observed. In this amplifier system, the input beam was configured with a cross section of ~1 cm^2 ($8 \times 12\ mm^2$) through a 33 cm amplifier cell. It was then focused into the oscillator cell with a 14 cm focal length lens. Although saturation in the amplifier cell allows attenuation to be added in front of the oscillator cell without a great penalty in energy efficiency, it was not found to be necessary up to an input energy of 3 J in a pulse width of 13 ns.

3. Relay imaging to the SBS cell

A highly relayed optical system, as described in previous sections, is essential for the successful operation of a phase conjugated amplifier system. As wavefront aberration accumulates on the laser pulse circulating in the amplifier, the system optics must collect, relay, and deliver to the SBS cells all components of the aberrated beam. In addition to this, we have found that the irradiance spatial profile delivered to the SBS oscillator is also significant. It is important that aberrations on the wavefront not be allowed to free propagate, producing a distorted irradiance spatial profile. The near field reproduction in the SBS conjugator return is observed to be poor for a strongly modulated input irradiance profile. If the distorted phase information is lost to near field distortion in the beam, then this poor near field reproduction will degrade the phase conjugation fidelity of the SBS mirror. By image relaying the amplifier aperture to the focusing lens of the SBS oscillator, a smooth spatial profile is presented to the phase conjugator. Any errors in the near field irradiance distribution in the SBS return in the form of small amplitude modulation are then corrected by gain saturation in the final amplifier passes.

4. SBS energy efficiency

It is also important to operate the SBS phase conjugator high above threshold to have high reflectivity and the best reproduction of the temporal profile of the input pulse. The energy efficiency of the phase conjugate mirror is determined primarily by the leading edge portion of the input pulse that is transmitted through the cells and lost before the SBS threshold is reached. For this reason, maximizing the SBS efficiency also optimizes the temporal reproduction fidelity of the input pulse. Figure 5 shows the reflectivity vs. input energy for the described two cell amplifier / oscillator configuration up to the nominal operating input level of 2.5J. The reflectivity saturates at a maximum value of 88% beyond ~1J. The insertion loss into the amplifier is very small with this high value of the SBS conversion efficiency and virtually no pulse shortening or steepening of the leading edge of the output temporal profile is observed.

5. SBS medium purity

The purity of the SBS medium is very important with respect to minimizing both optical absorption and the possibility of optical breakdown at the focus of the SBS oscillator. The removal of dissolved impurities which can undesirably increase absorption can normally be accomplished by distillation techniques. In practice, however, we have determined that in the case of CCl_4, it is sufficient to use the commercially available 99.9% spectroscopic grade liquid. However, a more challenging problem was found to be the presence of suspended particulate impurities which, when intercepted by the focused input beam, lead to a significantly reduced optical breakdown threshold. The most effective way of removal of these particles has been found to be the use of a closed loop filtration system installed on the SBS oscillator cell. A small centrifugal pump of stainless steel and teflon construction is used to circulate the CCl_4 through a 0.1 μm filter. Once the cell has been adequately filtered, it is not necessary to operate the circulation system during operation of the laser amplifier. After filtration, the optical breakdown

threshold for the 10-15ns input pulses is increased from ~40 mJ to over 1 J for the single cell focused SBS oscillator.

D. Laser system performance

In this section we will provide details on the overall performance of the laser system. At present it operates very reliably at up to 25J/pulse with a 13ns pulse length and repetition rates now in the range of 5Hz. The beam quality is approximately 1.25 times the diffraction limit.

1. Average power operation

In the present configuration of this flashlamp pumped Nd:glass amplifier system, the lamps can be pulsed at repetition rates of up to 5Hz with 2.5 kJ deposited electrical energy per pulse before reaching the stress fracture limit of the amplifier glass. When the laser amplifier system is operated in the SBS phase conjugated configuration, the near field irradiance distribution and far field divergence is maintained up to this full pulse repetition frequency. In fact, in an experiment in which the amplifier slab was intentionally thermally loaded at 6Hz, near diffraction limited output divergence was preserved up to the last laser pulses before the slab fractured. The amplifier system has been operated for extended periods with average output powers exceeding 100 W. Figure 6 illustrates a 1hr record of the energy of each of over fourteen thousand laser pulses with 27-28J/pulse and a repetition frequency of 4Hz. The temporal profile of the amplified output pulses is characterized by a smooth, unmodulated envelope without a steep leading edge that would be characteristic of significant temporal reshaping in the phase conjugator. The plot of a single temporal waveform as well as that of ~1800 superimposed waveforms collected at 4 Hz are shown in Figure 7.

New Nd doped phosphate glass compositions are presently being investigated which exhibit increases in thermal fracture strength of up to 2.5X over that of the glasses presently in use in this system. An increase in the thermal fracture limit of glass slabs has also been demonstrated by ion diffusion strengthening of the laser glass.[9] Our observations in past experiments has indicated that this process of placing the glass surface in compression by exchanging lithium ions with either sodium or potassium ions often results in the introduction of passive wavefront error in the finished slab. It is anticipated, however, that the wavefront correction provided by the SBS phase conjugator can accommodate this additional distortion. Finally, it has been recently demonstrated that the pulse repetition frequency can be increased by approximately a factor of two with the same size induced optical aberrations when the flashlamp excitation of this amplifier head is replaced by diode laser array pumping.[10] It is anticipated that with these advances, the average power of a glass amplifier system of this design will increase at least three fold to 300 W to 450 W.

2. Output beam quality

In order to extract high beam quality output from the phase conjugated amplifier system, a high quality input pulse must be provided. In ideal operation, the wavefront reversal achieved in the SBS phase conjugator allows the spatial phase distribution of the input beam to be reproduced in the amplified output beam. Using the single frequency self-seeded Nd:YLF oscillator, excellent seed beam quality has been measured with less than 1.1X the diffraction limited divergence as shown in Figure 8. The 25mJ output of this oscillator, however, must be further amplified and anamorphically expanded to provide the ~60 mJ, 8 x 120 mm input to the amplifier system. The divergence of this injected pulse is increased to 1.25X the diffraction limit in this process, primarily due to optical aberrations in the Nd:YLF preamplifier.

As the pulse repetition frequency of the laser system is increased, the thermal aberrations shown in Figure 4 result in significantly increased output divergence when the amplifier is operated in the unidirectional uncorrected mode without the SBS phase conjugate mirror. The measured output divergence vs. repetition rate is shown in Figure 9 for 25 J output pulses. At 3 Hz with an average output power of 75 W the divergence in the narrow beam dimension is increased to almost 15X the diffraction limit. However, when the amplifier system is configured as described previously with an SBS phase conjugator, the divergence does not measurably increase up to the maximum achievable pulse repetition frequency. Figure 10 compares the corrected and uncorrected far field profiles measured at the focus of a 120 cm corrected aspherical lens for 3 Hz, 75 W operation. With the phase conjugator, the width of the far field pattern is dramatically reduced to a single central peak with small side lobes characteristic of the angular distribution from a near uniformly filled aperture.

The 8 x 120 mm output of the amplifier system is characterized by smooth reproducible beam profiles. Figure 11 shows a CCD image of the near field output imaged at the external relay plane conjugate to the amplifier aperture. In order to quantitatively evaluate the measured divergence of the amplifier output, the theoretically expected diffraction limited divergence of a beam having the observed irradiance spatial distribution must be determined. A two-dimensional super-Gaussian distribution is first fitted to the near field profile. A comparison of this fit to cross sections of the measured profile is shown in Figure 11. The results of this numerical fit is then Fourier transformed to generate an expected far field distribution given a perfectly uniform phase profile. Figure 12 plots the predicted and experimentally measured far field patterns for the horizontal and vertical dimensions. It is found that if the divergence scale for the measured data is reduced by a factor of 1.25, nearly exact overlap of the calculated and measured profiles results. It is significant to note that this is the same divergence measured for the input pulse to the amplifier as illustrated by the overlay of the far field profiles of the input and amplified output beams in Figure 13. It is concluded therefore that the beam quality of the high power output is presently limited by that of the low power input.

The results of the analysis of the far field images indicate that there is a far field output lobe whose width is 1.25X that expected for a diffraction limited beam. However, it is important to determine what fraction of the measured output energy is contained in this narrow peak. There is the need to rule out the possibility that high spatial frequency irradiance or phase modulation is scattering a significant but undetected portion of the radiation into larger divergence angles. The dynamic range of the CCD cameras is such that a very low irradiance distributed evenly across the image background could fall below the signal-to-noise detection limit of the camera but still account for a significant fraction of the total output power. A straightforward measurement that can be made in this regard is the transmission of an aperture placed at the focus of the analysis lens. In this case an aperture was chosen that was 0.5 mm in diameter corresponding approximately to the distance between the first minima in the horizontal dimension of the measured far field profile. The expected transmission of this "bucket" for a 1.25X diffraction limited beam is calculated to be 96%. As illustrated in Figure 14, a transmission of ~92% was measured across the range of output energies up to 25 J. This 5% reduction in the expected transmission is reasonable based on the fact that the fit between the super-Gaussian and measured near field profiles shown in Figure 11 is not perfect. The small scale irradiance modulation on the beam profile is expected to contribute to a small reduction in Strehl, as was observed in the measurements.

E. Conclusion - laser for proximity print lithography

We have designed and constructed a Nd:glass amplifier system incorporating a SBS phase conjugate mirror which operates at 25-30 J/pulse with a pulse width of 13 ns FWHM and a pulse repetition frequency of 5 Hz. This results in a peak power of 2 GW and an average output power that significantly exceeds 100W. The divergence of the system is measured to be 1.25X the diffraction limit and the output can be frequency doubled with an efficiency of 82% at full average power. The laboratory prototype has proven to be an extremely reliable system and is presently in use as a laser source for a number of experimental investigations including Raman beam conversion[11], X-ray generation from laser produced plasmas, and high energy SBS pulse compression.[12]

The laser system has been thoroughly tested with over 10^6 shots and we have designed a compact package which easily fits the allocated profile on an x-ray lithography stepper. The introduction of this laser design into the commercial x-ray lithography market has now begun.

III. 0.5 J/pulse diode-pumped Nd:YAG laser for soft x-ray projection lithography

A. Soft x-ray projection lithography

Projection lithography using soft x-rays (SXPL) offers the potential for ultra-fine resolution lithography, down to 0.2 μm and lower. The concept was first proposed by Hawryluk and Seppala[13] and Silvfast and Wood[14] nearly 5 years ago. Since that time there has been significant progress towards developing the basic principles and technologies. In the concept, schematically shown in Figure 15, soft x-rays near the 130 Å

region with a bandwidth of approximately 3 Å are generated from a point source. This wavelength choice results from the existence of high performance narrowband multilayer optics at 130 Å, a wavelength just longer than the silicon L-edge. The x-ray source is proposed as a laser produced plasma generated by the interaction of laser light of intensity greater than 10^{11} W/cm^2 with a high Z target material. As shown in the figure, x-rays from the target are efficiently collected by a pair of multilayer-coated condenser mirrors. The condenser mirrors project the narrowband radiation onto a mask or master-reticle which works in reflection. The mask is a thin, IC metallization pattern over a multilayer coating which, in turn, is supported by a flat, highly polished, massive substrate. The radiation pattern reflected from the mask is imaged by a high precision, four mirror imaging system. While there are a number of different designs for the imaging optical system[15], it generally can be characterized as follows: it is a ring-field imaging system providing for step and scan exposure of the wafer; an f# of f/6 or smaller will provide resolution of <0.1 μm at the wafer; it will project a virtually distortion-free imaging over the ring-field (distortion <0.01 μm at the wafer); and it will be a demagnifying system with a reduction factor of approximately 5X.

A significant amount of work remains to be done to field a commercial quality system. This includes the fabrication of precision aspherical mirrors and the mechanisms to align and rigidly hold them, the production of a high quality imaging resist, and an alignment and registration system capable of supporting the very fine printed features. It also involves the development of a compact, high efficiency, high average power laser source to generate the laser plasma.

B. Laser system for SXPL

We are currently working on the development of a diode pumped solid state laser as part of a soft x-ray lithography system being assembled at LLNL. The laser for this system has been designed to a set of specifications appropriate for generating x-ray radiation at 130Å. The specifications for the laser are 0.5 J/pulse, 5 to 7.5 ns pulse length, and a 1.3 kHz repetition rate.

In order to build a laser meeting these specifications, we have used an appropriately scaled version of the master oscillator/regenerative amplifier technology discussed previously for proximity print lithography. The oscillator for this device is a self-seeded Q-switched Nd:YAG rod pumped by an array of laser diodes. The power amplifier is also Nd:YAG in the form of a slab pumped by two large arrays of laser diodes with a small signal amplification design goal of 16 per pass. As in the previously described design, high beam quality and high extraction efficiency will be maintained in this device through the use of an SBS phase conjugator placed at the mid transit point in the amplifier. The amplifier is configured to use passive polarization switching but because of the higher amplifier gain, only 4 amplifier passes are required for efficient extraction and consequently the phase conjugate mirror is positioned after the second amplifier pass.

The high repetition rate of the laser diode pumps is achieved through the use of an aggressive heat rejection concept using silicon microchannel coolers.[16] These coolers can maintain acceptable diode operating temperatures while rejecting heat at rates up to 1 kW/cm^2. Each cooler consists of a silicon package on which two 0.9 mm long diode bars are mounted. These are then stacked at a density of 10 packages per cm with a single water inlet and outlet. Each package requires a cooling flow of 1 cm^3/s with a pressure of 60 psi. In this configuration each 1.8cm wide diode package is capable of 100 W peak power output. No reduction in this peak power is observed at a duty cycle of up to 25% resulting in an average power of 25 W/package and a diode array average pumping irradiance of 140 W/cm^2.

C. *Pre-prototype SXPL laser experiments*

As a major step in developing this laser, we have constructed a pre-prototype master oscillator/regenerative amplifier system using available hardware and have completed critical testing at the full amplifier thermal load. The pre-prototype amplifier used an existing diode pumped Nd:YAG head which has been demonstrated at 1 kW average power output when configured as a free running oscillator with a stable resonator.[17] The head has a zig-zag slab with nearly square tipped ends and is consequently limited to a small signal single pass gain of approximately 1 Np corresponding to a stored energy of 370 mJ.

1. Optical layout

To efficiently extract at this low gain, an eight pass optical configuration using the same design principles from the proximity print laser was used. A flashlamp pumped Nd:YAG Q-switched oscillator was used for these pre-prototype experiments, prior to the completion of the high repetition rate diode pumped oscillator. It was a self-seeded single frequency oscillator with 8 ns output pulses at a maximum repetition rate of approximately 20 Hz. However, in order to test the performance of the laser with the amplifier head under full thermal load, the diode pump arrays were operated at repetition rates up to 2.3kHz with the oscillator input synchronized to extract approximately 1 pulse out of each 100.

The layout for this experiment is shown in Figure 16. The amplifier slab had a highly reflective coating on the back face and was aligned in a three diamond zig-zag reflection scheme. In this case a beam at the appropriate input angle reflects from the slab pump faces three times to reach the back face where it reflects and zig-zags back out. In this test setup, the regenerative amplifier consisted of an 8 pass layout with a Faraday rotator used to passively switch the polarization for the output beam. A 1:1 telescope was used to relay image the beam between the amplifier and the SBS cell and a $\lambda/4$ rotator was placed between passes of the amplifier to direct the beam to the phase conjugate mirror after four slab passes. In this setup, the ~80 mJ incident at the SBS mirror was lower than that for the previously described 25 J laser by over an order of magnitude so a single cell SBS phase conjugate mirror worked well.

2. Energy storage and depolarization

A detailed series of tests was completed in order to characterize the operation of the diode pumped slab for use as an optical storage amplifier. Figure 17 shows, at the low repetition rate of 10 Hz, the measured slab gain as a function of diode pulse duration. For this nearly rectangular shaped slab with no ASE edge claddings, the gain clamps at approximately 1 Np (single pass small signal amplification of 2.6, 7.0 double pass). Figure 18 shows the extracted energy vs. oscillator input energy for this storage level. An output of 180 mJ was obtained with an 8 mJ input pulse corresponding to 55% extraction efficiency, assuming a value of the saturation fluence, E_{sat}, of 660 mJ and 87.5% slab fill.

As the amplifier repetition rate was increased, a drop in the amplifier gain was observed, as illustrated in Figure 19. This was determined to be caused by a spectral shift in the diode pump arrays as their thermal load increased. The increased temperature of the diodes shifted the output spectrum and decreased the overlap with the Nd:YAG absorption features around 808 nm. This problem has been remedied in the new array of diodes being assembled for the prototype laser. By tailoring the emission spectrum to be slightly blue shifted from the peak absorption with no thermal load applied, the diode output shifts into near optimum overlap at full repetition rate.

A second limitation encountered in the pre-prototype experimental investigations was an increasing level of depolarization of the beam transmitted through the amplifier as the diode pumping duty cycle was increased. Figure 20 shows the measured average depolarization over the 3 x 14 mm extraction aperture as the diode pulse width and consequently the pumping duty cycle was increased. At 23% duty cycle the depolarization loss reached ~12%. We have extensively modeled the source of this effect using a three dimensional code which, given the material constants, slab geometry, and thermo-mechanical boundary conditions, numerically solves for the temperature, stress, and deformation distributions within the slab. Zig-zag path optical rays can then traced through the thermally loaded medium resulting in a map of wavefront distortion and depolarization for the amplifier aperture.[18] The prototype design will include longitudinal cooling water flow and areas of tailored thermal conductivity near the slab tips to maximize the thermal uniformity and minimize the stress and consequent optical depolarization in the slab.

3. Output beam divergence

A critically important aspect of the laser performance will be the beam quality of the output under full thermal load. Beam quality is important not only for optimizing extraction efficiency and minimizing the potential for optics damage resulting from beam distortions, but it is also necessary for the efficient generation of x-rays. Although the required focused spot size on the target is not at the diffraction limit of the laser divergence, the irradiance pattern is required to exhibit a smooth spatial profile in a single well defined lobe. As in our other laser designs, an SBS phase conjugator plays an important role in the control of beam quality by correcting thermally induced optical

aberrations in the gain medium. In fact, the strongest motivation to perform these pre-prototype extraction experiments came from a desire to demonstrate that the slab aberrations under full thermal load could be adequately compensated in our MOPA extraction scheme.

To qualify and quantify the aberrations in the thermally loaded slab, the far field pattern of the extraction beam after four passes through the slab was examined. As illustrated in Figure 21, these patterns represent the wavefront distortions that were present in the beam incident on the phase conjugate mirror. Results are shown for no thermal loading (0 Hz), intermediate loading (1000Hz) and full thermal loading (2300 Hz). These points correspond to cooling rates at the slab faces of approximately 0, 15, and 34 W/cm^2, respectively. In addition to the obvious distortion in the far field, the wavefront acquires 2.5 mrad of vertical tilt per 3-diamond pass due to the temperature rise of the slab cooling water which has a flow direction perpendicular to the optical axis. However, when the system is operated with the SBS phase conjugate mirror using the full 8 gain passes, these errors are completely corrected. Figure 22 shows near diffraction limited divergence for amplified outputs ranging between 10 Hz and the full thermal load at 2.3 kHz. The effect of the tilt introduced by the amplifier is eliminated and no variation in the far field pattern with increasing diode pump repetition rate is observed.

D. Prototype SXPL laser design

The new amplifier and slab hardware have been designed and are expect to provide 3 Np of gain per pass. With the higher gain, only 4 slab passes are required to obtain good extraction efficiency. Figure 23 shows the modified optical layout of the prototype design. This design uses a waveplate to induce a 90° polarization rotation at the SBS cell, eliminating the need for a Faraday rotator or Pockels cell to switch out the amplified output. The oscillator beam is shaped to the slap aperture dimensions by a rectangular mask which is relay imaged to the amplifier. After two gain passes, the extraction beam is relayed to the phase conjugator. The SBS output then retraces its path, extracting the major portion of the amplifier stored energy in a final two slab passes. The oscillator is a diode-pumped Q-switched single frequency Nd:YAG rod laser emitting ~5 mJ 8 ns pulses at a repetition frequency of 1.3kHz. It is end pumped by a diode array cooled in the same manner as the slab pump arrays but incorporating cylindrical microlenses mounted onto each diode bar. The resulting low diode divergence output is delivered to the end of the rod by a tapered lens duct.

Fabrication and assembly of the laser system is nearing completion. The slab pump diode arrays have been assembled and tested at 15 kW peak power with up to a 20% duty factor. The full repetition rate master oscillator has been assembled and is in the testing phase. Final testing will answer remaining questions not addressed in the pre-prototype experiments such as the average power handling capability of the SBS mirror and other sensitive optical components such as the polarizing beam splitters.

IV. 1 kJ/pulse Nd:glass laser driver for x-ray lasers

A. The x-ray laser

Lasers operating at x-ray wavelengths have been pursued since the early 1970s. Conclusive demonstration came in the mid-1980s by groups working independently at Princeton and Livermore.[19] The goals of the current research efforts include that of developing the x-ray laser from a scientific curiosity into a laboratory tool with all the utility of the optical laser. In general x-ray lasers now operate from ~33 to 3.5 nm, can produce up to 10 mJ of energy in pulse lengths from 0.1 to tens of ns, have measured linewidths of $\geq 5 \times 10^{-5}$, typically have a divergence of 1 to 10 mrad (much larger than diffraction limited), and have measured brightness values that are five to eight orders of magnitude greater than that of synchrotrons or undulators. Important issues for continued development include the lack of multilayer mirrors which function at normal incidence with reasonable reflectivity for wavelengths less than 13 nm and the lack of dedicated, small-size, low-cost facilities for developing the x-ray laser and its applications. We describe here our efforts toward the development of a compact high power laser source with repetition rate capability specifically designed to further the development and applications of x-ray lasers.

B. The x-ray laser driver design

The x-ray laser driver requires a single pulse energy of >1 kJ with a pulse length of <1 ns for efficient x-ray production. In addition, a repetition rate of 1 Hz for at least 200 shots is required to produce an x-ray source competitive with the output of a synchrotron. Finally a compact laser is desirable for industrial applications. The high storage capacity of glasses having moderately low cross sections for stimulated emission is well suited for this application. A heat capacity zig-zag slab power amplifier is used to generate the high pulse energies in a compact laser system. In the heat capacity mode of operation, the laser slab is uncooled during its 200 shot operation. The slab can heat up during its operating cycle until the temperature rise produces a laser state population redistribution which reduces the observed gain. Since the slab is not actively cooled, the thermal stress which would normally lead to slab fracture is greatly reduced. Consequently, the total extracted energy during an operation cycle of a heat capacity laser can be up to 5 times larger than for a similar cooled laser operating in steady state for the same time period. To avoid self focusing damage in the slab, a long pulse length is used to extract the stored energy. After output an SBS pulse compressor is used to produce the desired 1 ns pulse duration.

The x-ray laser driver design is a MOPA utilizing a optically segmented slab in a modified ring architecture. The conceptual layout is presented in Figure 24. The design criteria used here are similar to those used in the previously described laser systems. This system similarly employs a phase conjugator for good beam quality and prevention of optics damage, a fully relayed optical train, and a compact ring style layout. A single set of optics is used to relay the beam through multiple slab passes, but in this design, the beam transverses a different segment of the slab on each pass for increased extraction

efficiency. The slab size 56 x 60 x 4 cm^3 and stores 4.8 kJ with a single pass small signal amplification factor of 25. Numerical modeling projects 1.5 kJ optical extraction in a 30-50 ns pulse.

The master oscillator will be required to output a 5mJ TEM_{00} output beam with a single longitudinal mode in a 30-50 ns pulse. Pulse shaping can be carried out on the low power master oscillator output to offset undesirable gain saturation pulse reshaping during amplification. The beam is enlarged to a rectangular beam of 6x30 cm^2 and is injected into the multi-pass slab amplifier where it makes three amplifier passes before reaching the SBS phase conjugator. Between each gain pass the anamorphic telescope reduces the beam width by a factor of 2.5 along one dimension.

Approximately 11 J will be directed into the phase conjugate mirror and, as in the case of the 25 J proximity print x-ray lithography system, it will use an SBS focused oscillator with a collimated SBS amplifier. This design allows most of the incoming energy to be reflected in the amplifier cell, effectively shielding the focused oscillator cell from the peak input power. Approximately 80% reflectivity is expected, however, the efficiency of the phase conjugator is not an important issue since only a small portion of the energy stored in the amplifier is extracted before that point. The conjugated output beam retraces its path through three additional gain passes. The beam is now expanded by a factor of 2.5 between each pass as it saturates the gain. The optical transit system is fully relay imaged to insure that aberrations imposed on the beam are delivered to and can be compensated by the SBS phase conjugator.

Damage resulting from nonlinear self-focusing is a significant problem in compact high power laser systems. To avoid this damage, a 30-50 ns pulse is used for the laser extraction. The resulting B-integral, a scaled product of the nonlinear index and optical irradiance integrated over the propagation distance,[20] is similar in magnitude to that predicted for the 25 J proximity print x-ray lithography laser system. Shorter pulses would result in the possibility of slab damage. In designing this system it is important to consider the contribution to the B-integral by the amplifier glass as well as that of the SBS medium.

The 1.5 kJ, 30-50 ns output pulse is coupled out of the amplifier system by a thin film polarizer and is directed into an SBS pulse compressor consisting of a focused oscillator and a large aperture amplifier. Approximately 1 J is split off the main beam and focused into an SBS oscillator cell. The Stokes shifted output from the oscillator is then amplified and temporally compressed in the SBS amplifier which is pumped by the remaining high power beam. The compressed 1 kJ, 1 ns output pulse can then be line focused into the target vacuum chamber to produce a coherent, high repetition rate, x-ray source.

C. *Pre-prototype laser development*

Our program's current focus is directed toward demonstrating the key technologies required to develop this kJ x-ray laser driver. Specifically, we have designed, built and are currently testing a subscale heat capacity laser system, having the same gain and

thermal loading as that required for the 1.5kJ laser described above. The subscale laser slab, which is $20 \times 24 \times 2\ cm^3$, will produce 150J output in a 40 ns pulse. The laser extraction optical layout is identical to that described in Figure 24. Activating this subscale system will fully demonstrate heat capacity laser operation, SBS phase conjugation at high energies, and the previously described ring optical architecture. Another key technology yet to be demonstrated is SBS pulse compression at the required high pulse energies. We are presently performing pulse compression experiments at 25 J with the proximity x-ray lithography system[12] and will integrate that hardware into the 150 J subscale testbed to produce 100 J 1 ns pulses. This output will be focused onto a target producing a Ge (23.2 nm) x-ray laser source operating at 1 Hz. Successful activation of this subscale laser system will fully demonstrate most laser engineering issues associated with a full-scale, short-wavelength, x-ray laser driver.

V. General conclusions

In this work we have described three different laser systems being developed for the generation of x-rays. Each of them depends on the correction of thermally induced aberrations on the extraction beams by the use of a conjugate mirror. The successful operation of these designs demonstrates the fact that SBS phase conjugation has advanced beyond the level of a curious nonlinear optical phenomenon to become a reliable component in high average power laser systems. The most notable improvement in laser performance resulting from the wavefront correction provided by the conjugator is the near diffraction limited output divergence. However, the phase conjugator also contributes to the reliability of the amplifier system by greatly reducing the optical alignment sensitivity and by providing interstage gain isolation between amplifier passes. We feel that the detailed considerations shared by the specific amplifier designs presented here are applicable in general to the design of high average power, high beam quality laser systems using SBS phase conjugation.

VI. Acknowledgements

We would like to aknowledge the invaluable technical assistance of B. Bhachu, R. Bonner, P. Keiser, W. Manning, S. Mitchell, P. Reichert, and J. Wintemute of Lawrence Livermore National Laboratory without which this work would not have been possible. This work was performed under the auspices of the U. S. Department of Energy by Lawrence Livermore National Laboratory under Contract W-7405-Eng-48.

References

1. D. J. Nagel, M. C. Peckarer, R. R. Whitlock, J. R. Grieg and R. E. Pechacek, "Submicrosecond x-ray lithography,"Electron. Lett. 14, 781-782 (1978).
2. L. A. Hackel, C. B. Dane, M. R. Hermann, and L. E. Zapata, "Solid State Laser Driver for Projection X-ray Lithography," Optical Society of America Soft-X-Ray Projection Lithography Topical Meeting, May 3-6, 1992, Monterey, California.
3. L. A. Hackel, J. L. Miller, and C. B. Dane, "Phase Conjugation in a High Power Regenerative Laser Amplifier System," Int. J. Nonlin. Opt. Phys. 2, 171-185 (1993).
4. C. B. Dane, L. E. Zapata, W. A. Neuman, M. A. Norton and L. A. Hackel, "Design and Operation of a 100W Near Diffraction -Limited Laser Amplifier with SBS Wavefront Correction," submitted to IEEE J. Quant. Electron.
5. C. B. Dane, L. E. Zapata, and L. A. Hackel, "Long pulse regenerative amplifier architecture with near diffraction-limited output divergence," Conference on Lasers and Electro-Optics, CWI1, Baltimore, MD, May 2-7, 1993.
6. J. J. Ottusch and D. A. Rockwell, "SBS Phase Conjugation Fidelity Fluctuations," Opt. Lett. 16, 369-371 (1991).
7. C. B. Dane, W. A. Neuman, and L. A. Hackel, "Pulse-shape dependence of stimulated-Brillouin-scattering phase-conjugation fidelity for high input energies," Opt. Lett. 17, 1271-1273 (1992).
8. G. J. Crofts and M. J. Damzen, "Experimental and theoretical investigation of two-cell stimulated-Brillouin-scattering systems," J. Opt. Soc. Am. B 8, 2282-2288 (1991).
9. J. E. Marion, "Strengthening of Laser Slabs," Laser Program Annual Report, Lawrence Livermore National Laboratory, Livermore, CA, UCRL 50021-87 (1987).
10. G. Dube, H. Morris, T. Dellamano, J. Hollister, J. Powers, L. Long, A. Reynolds, J. Abate, E. Miller, and J. Forsyth, "700 kilowatt diode pumping system," Conference on Lasers and Electro-Optics, CPD7, Baltimore, MD, May 2-7, 1993.
11. M. R. Herman, M. A. Norton, L. A. Hackel, and D. Twede, "Efficient high power Stokes and anti-Stokes Raman frequency generation via polarization tuning enhancement," Conference on Lasers and Electro-Optics, CThD2, Baltimore, MD, May 2-7, 1993.
12. C. B. Dane, L. A. Hackel, and W. A. Neuman, "High Energy Pulse Compression," submitted to IEEE J. Quantum Electron.
13. A. M. Hawryluk and L. G. Seppala, "Soft x-ray projection lithography using an x-ray reduction camera," J. Vac. Sci. Technol. B 6, 2162-2166 (1988).
14. W. T. Silfvast and O. R. Wood II, Microelectron. Eng. 8, 3 (1988).
15. N. M. Ceglio, A. M. Hawryluk, D. G. Stearns, D. P. Gaines, R. S. Rosen, and S. P. Vernon, "Soft x-ray projection lithography," J. Vac. Sci. Technol. B 8, 1325-1328 (1990).
16. D. Mundinger, R. Beach, W. Benett, R. Solarz, W. Krupke, R. Staver, and D. Tuckerman, "Demonstration of high performance silicon microchannel heat exchangers for laser diode array cooling," Appl. Phys. Lett. 53, 1030-1032 (1988); R. Beach, D. Mundinger, W.

Benett, V. Sperry, B. Comaskey, and R. Solarz, "High-reliability silicon microchannel submount for high average power laser diode arrays," Appl. Phys. Lett. 56, 2065-2067, (1990).

17. B. J. Comaskey, R. Beach, G. Albrecht, W. J. Benett, B. L. Freitas, C. Petty, D. VanLue, D. Mundinger, and R. W. Solarz, "High Average Power Diode Pumped Slab Laser," IEEE J. Quant. Electron. 28, 992-996 (1992); B. Comaskey, G. Albrecht, R. Beach, S. Sutton, and S. Mitchell, "1000-W diode-pumped folded zigzag slab laser," Conference on Lasers and Electro-Optics, CWI5, Baltimore, MD, May 2-7, 1993.

18. The computer code TECATE numerically solves for the temperature, stress, and deformation distributions and BREW calculates the transmitted optical wavefront. These codes were originally developed for use in the NOVA project by Lawrence Livermore National Laboratory scientists R. J. Gelinas and S. K. Doss. Time dependence in the thermal computations and a generalized surface source simulating lamp or diode laser pumping were later implemented in TECATE by S. K. Doss, J. A. Blink, and L. E. Zapata to accommodate zigzag amplifiers such as this one.

19. D.L.Matthews, P.L. Hagelstein, M.D. Rosen, M.J. Eckart, N. M. Ceglio, A. U. Hazi, H. Medecki, B. J. Macgowan, J. E. Trebes, B. L. Witten, E. M. Campbell, C. W. Hatcher, A. M. Hawryluck, R. L. Kaufman, L. D. Pleasance, G. Rambach, J. H. Scofield, G. Stone, and T. A. Weaver, *Phys. Rev. Lett.* **54**, 110 (1985); S. Suckewer, C. H. Skinner, H. Milchberg, C. Keane and D. Voorhees, *Phys. Rev. Lett.* **55**, 1753 (1985).

20. W. L. Smith, "Nonlinear refractive index," Handbook of Laser Science and Technology, M. J. Weber, Ed. (CRC Press, Inc., Boca Raton, Florida, 1986), vol. 3, pp. 259-264.

Figures

1. A schematic diagram of a proximity print x-ray lithography setup. A high energy laser is focused onto a target generating x-rays which pass through an exposure column and print circuit of a mask onto a resist coated silicon wafer . Approximately 10 to 50 mJ/cm^2 of x-ray flux is required.

2. A schematic of the regenerative amplifier geometry incorporating an SBS phase conjugate mirror. A passive 90∞ rotator in the regenerative amplifier ring causes the injected pulse to make two ring passes (4 slab passes) before it is directed into the phase conjugator. The SBS wavefront reversed return then retraces the input path for an additional two ring passes, for a total of 8 gain passes, before it exits and is isolated from the input pathway by a Pockels cell.

3. The Nd:glass slab design used in the proximity print laser amplifier system. The input and output faces are parallel and are oriented 1.5° from normal. An ASE absorbing edge cladding is attached to the top and bottom edges of the slab using an index matching polyurethane elastomer.

4. An illustration of the SBS phase conjugation process. We believe that optimal wavefront reversal fidelity results from optically relaying the amplifier aperture to the focusing lens of the conjugator and from operating the conjugator high above threshold.

5. (a) The experimentally measured reflected energy versus input energy for the two cell SBS phase conjugator arrangement. (b) The same data plotted as SBS reflectivity versus input energy.

6. A 1 hr record of the energy of each of over fourteen thousand laser pulses with 27-28 J/pulse and a repetition frequency of 4 Hz. The dashed line marks an average output power of 100 W.

7. The plot of (a) a single temporal waveform as well as (b) that of ~1800 superimposed waveforms collected at 4 Hz. The overlaid pulses were accumulated in the infinite persistence mode of a digital storage oscilloscope.

8. Experimentally measured (a) near and (b) far field irradiance profiles for the 25 mJ single frequency Nd:YLF oscillator. The measurements were made after the beam had been expanded by a telescope with a magnification of 1.5, just prior to its amplification in the 4 mm Nd:YLF preamplifier. The results indicate a divergence of less than 1.1X the diffraction limit.

9. The measured output divergence in the narrow beam dimension vs. repetition rate for 25 J output pulses. At 3Hz, with an average flashlamp power of 7.5 kW, the divergence is increased to almost 15X the diffraction limit.

10. A comparison of the far field profiles measured at the focus of a 120 cm lens for 3 Hz, 75 W operation (a) without and (b) with SBS phase conjugation. Plot (c) overlays horizontal cross-sections of both cases.

11. (a) CCD image of the near field output imaged at the external relay plane conjugate to the amplifier aperture. (b) and (c) show vertical and horizontal cross sections of this

profile, respectively. The smooth curve plotted with each cross section is the result of a super Gaussian fit to this near field profile.

12. (a) CCD image of the far field profile measured simultaneously with the near field profile shown in Fig. 11. A comparison between (b) vertical and (c) horizontal cross sections of this profile and the Fourier transform of the super Gaussian fit of the near field profile is shown. It is found that if the divergence scale for the measured data is reduced by a factor of 1.25, nearly exact overlap of the calculated and measured profiles results.

13. A comparison of horizontal cross sections of the far field profiles of the low energy input pulse (solid line) and the amplified output pulse (dashed line). The divergence is unchanged to within the uncertainty of the experimental measurement.

14. Transmission of a 0.5 mm aperture placed at the focus of a 120 cm focal length lens. The expected transmission of this "bucket" for a 1.25X diffraction limited beam was calculated to be 96%. A transmission of ~92% was measured across the range of output energies up to 25 J.

15. Schematic representation of a 5X reduction, ring field scanning system employing four imaging mirrors, a reflective mask, two condenser mirrors, and driven by a laser produced "point" source of x-rays.

16. A schematic diagram of the 8 pass optical regenerative amplifier system used to verify the concepts for the full power prototype design concepts. This setup uses a Faraday rotator to separate the input and output whereas the prototype design uses a higher gain 4 pass angle multiplexed design, as shown in Figure 23.

17. Measurement of gain versus diode pulse width (equivalent to input energy) for the square tipped Nd:YAG slab used in the pre-prototype experiments. The data was taken at low repetition rate and the roll-over of the single pass gain at 1 Np is evidence of the ASE limitation of this square tip design without absorbing edge claddings.

18. Extracted output energy vs. oscillator input energy for the pre-prototype configuration. The conditions were 136 A diode pump current, 100 μs pump pulse width, 3 x 14 mm beam, 8 gain passes with SBS phase conjugation, 100 Hz amplifier PRF, 10 Hz oscillator PRF, and 8 ns input pulses.

19. Measured slab gain as a function of pulse repetition frequency. A laser probe pulse at the end of a 136 A, 100 μs diode pump pulse measures a reduction in storage efficiency of 20% at maximum duty cycle due to the spectral shift in the diode laser arrays. With a more optimal choice of starting wavelength (bluer) for the diode output, this drop-off will not occur.

20. Measured depolarization loss as a function of diode pulse width (i.e. pumping duty cycle) for the diode arrays operated at 136 A, 2300 Hz PRF. The average loss was measured over a 3 x 14 mm window with a 8 ns probe pulse at the end of the diode array pulse. Improved thermal management is expected to significantly reduce this loss in the prototype design.

21. (a) CCD far field image of the transmitted wavefront for 2 consecutive 3-diamond optical transits of the slab thermally loaded at 2300 Hz. (b) Line-outs of the far field image for

three repetition rates, 0 Hz, 1000 Hz and 2300 Hz. In addition to thermal distortion, the wavefront acquires up to 2.5 mrad of vertical tilt due to the cooling water temperature rise as it flows over the slab faces.

22. (a) CCD image of the far field of the amplified output using the phase conjugator. (b) line-outs of the far field data for 10, 500, 1000, 1500, 2000 and 2300 Hz amplifier PRF showing near diffraction limited beam quality and the correction of amplifier induced tilt at all repetition rates. The line-outs were scaled to the same peak value for the purposes of comparison.

23. Optical layout of the prototype SXPL laser. The new design will be operated at 2.5 to 3 Np of gain allowing a 4-pass setup which uses an angular multiplexing and eliminates the need for a polarization rotator.

24. Conceptual design of a 1 kJ solid-state laser for use as a pump for an x-ray laser. The design employs a master oscillator and multipass amplifier with full image relaying and mid-transit phase conjugation. The design is capable of 1 Hz repetition rate for 200 consecutive shots.

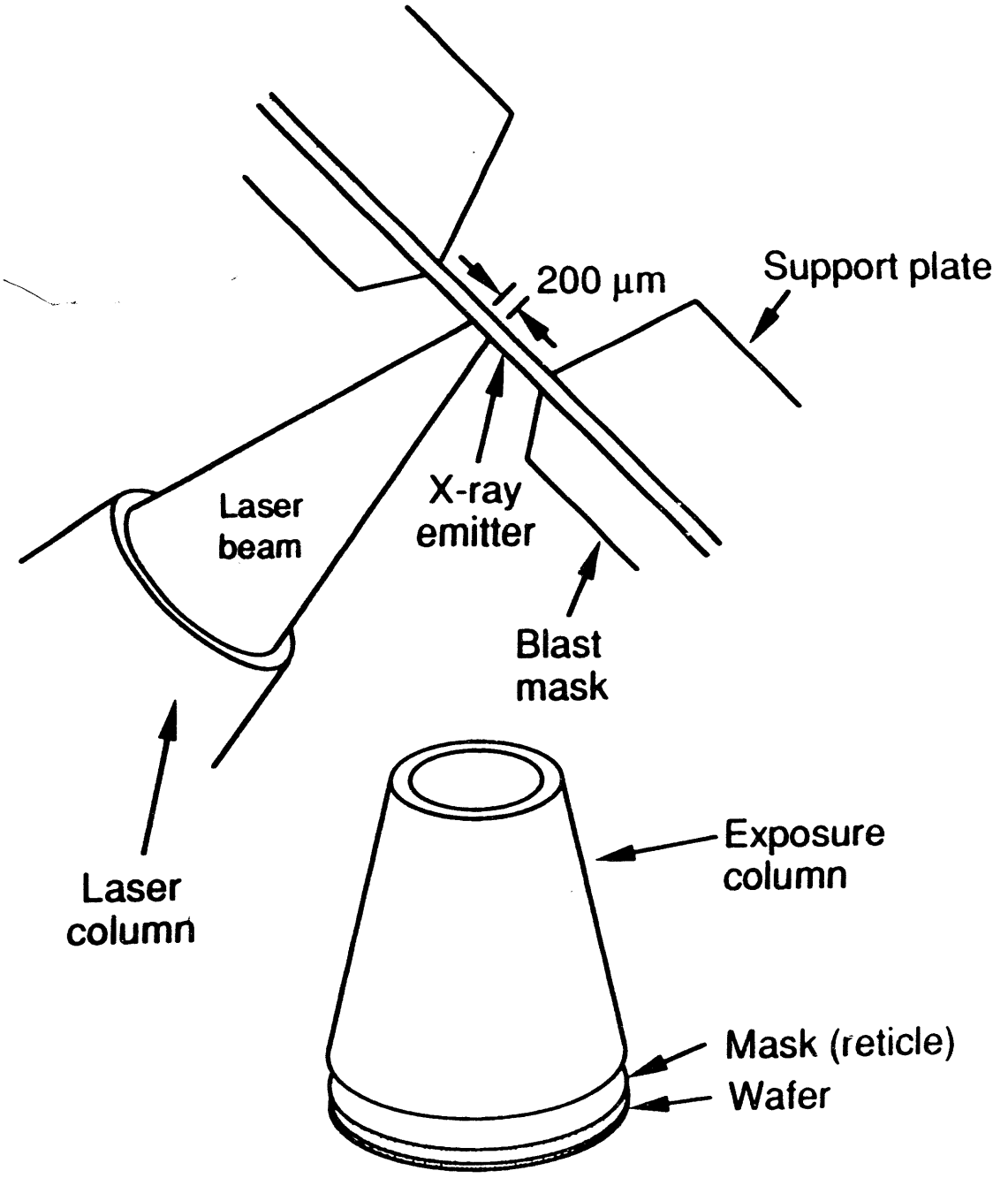
200 µm
Support plate
Laser beam
X-ray emitter
Blast mask
Laser column
Exposure column
Mask (reticle)
Wafer

Fig. 1

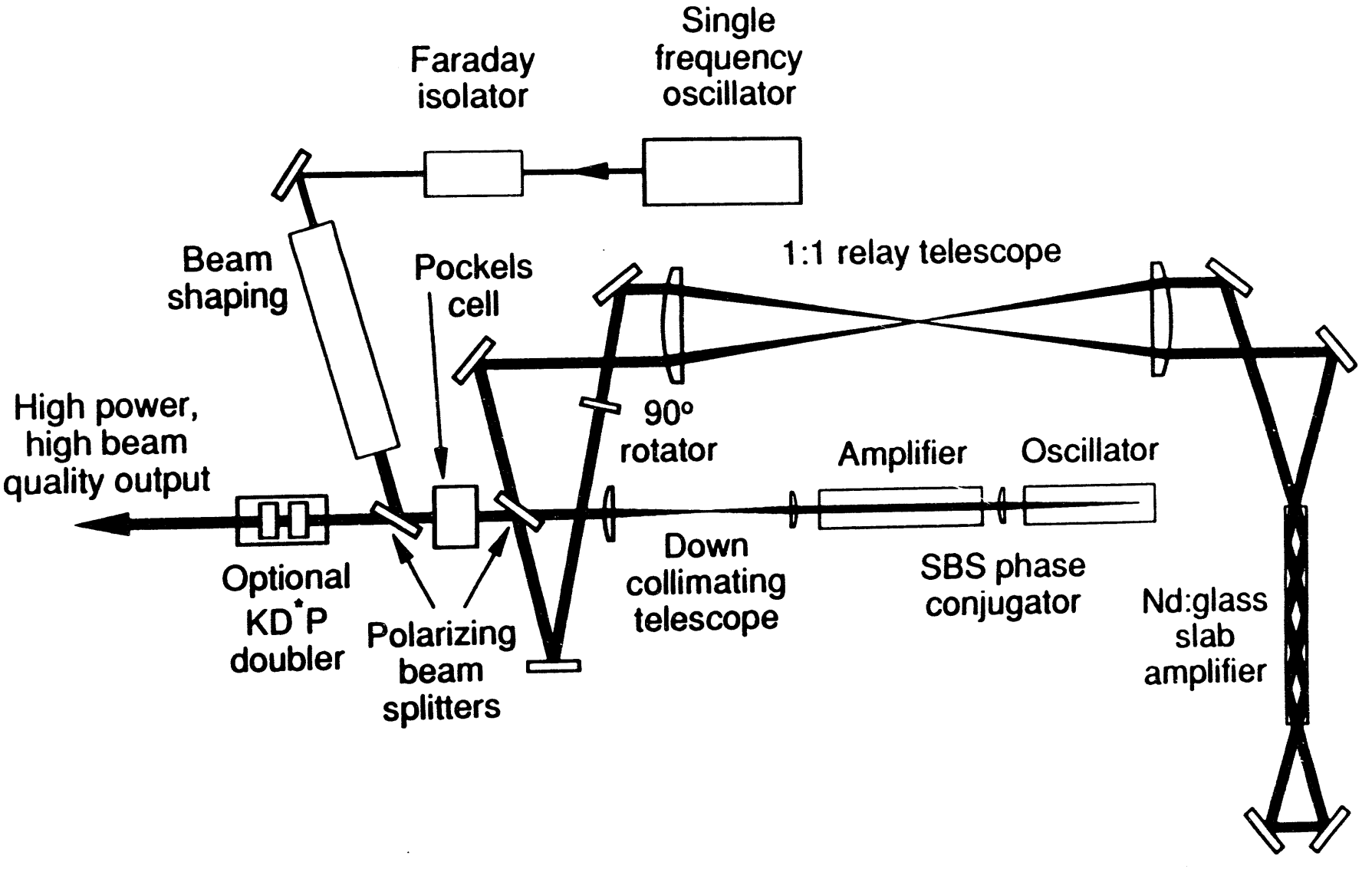
Single
frequency
oscillator
Faraday
isolator
Beam
shaping
Pockels
cell
1:1 relay telescope
High power,
high beam
quality output
90°
rotator
Amplifier
Oscillator
Optional
KD*P
doubler
Polarizing
beam
splitters
Down
collimating
telescope
SBS phase
conjugator
Nd:glass
slab
amplifier

Fig. 2

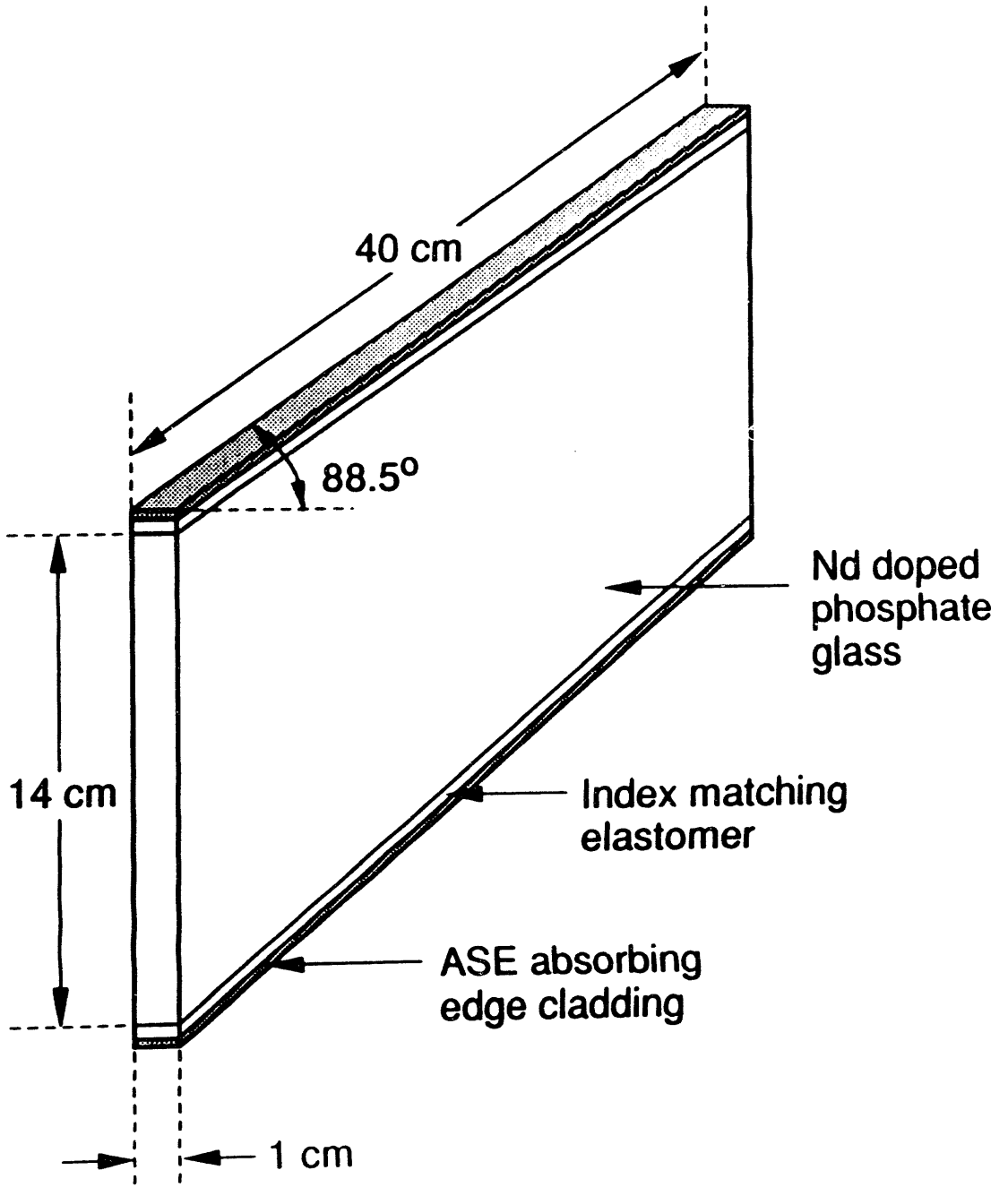
40 cm
88.5°
14 cm
1 cm
Nd doped
phosphate
glass
Index matching
elastomer
ASE absorbing
edge cladding

Fig. 3

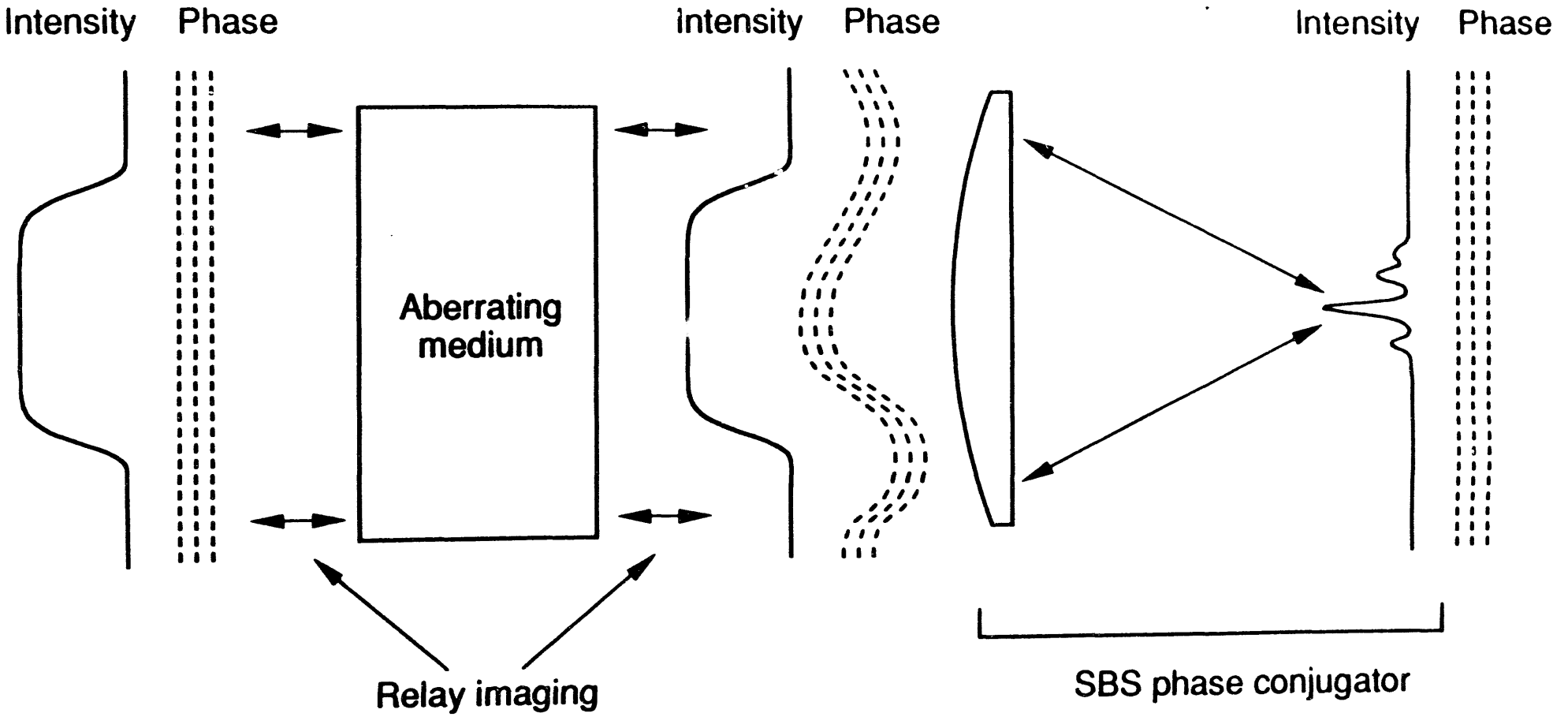
Intensity
Phase
Aberrating medium
Intensity
Phase
Intensity
Phase
Relay imaging
SBS phase conjugator

Fig. 4

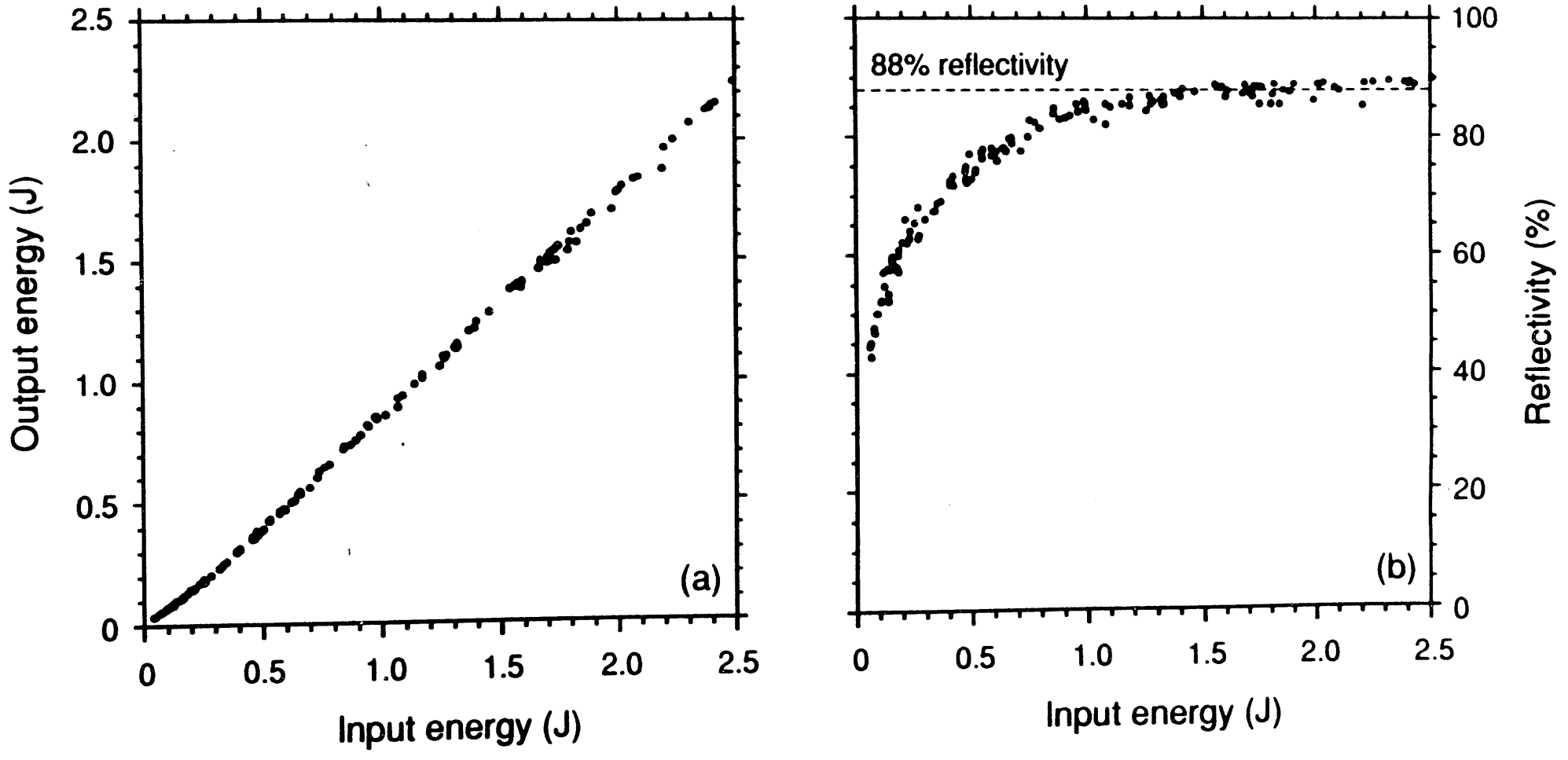
Output energy (J)
2.5
2.0
1.5
1.0
0.5
0
0
0.5
1.0
1.5
2.0
2.5
Input energy (J)
(a)
88% reflectivity
100
80
60
40
20
0
Reflectivity (%)
(b)
Input energy (J)

Fig. 5

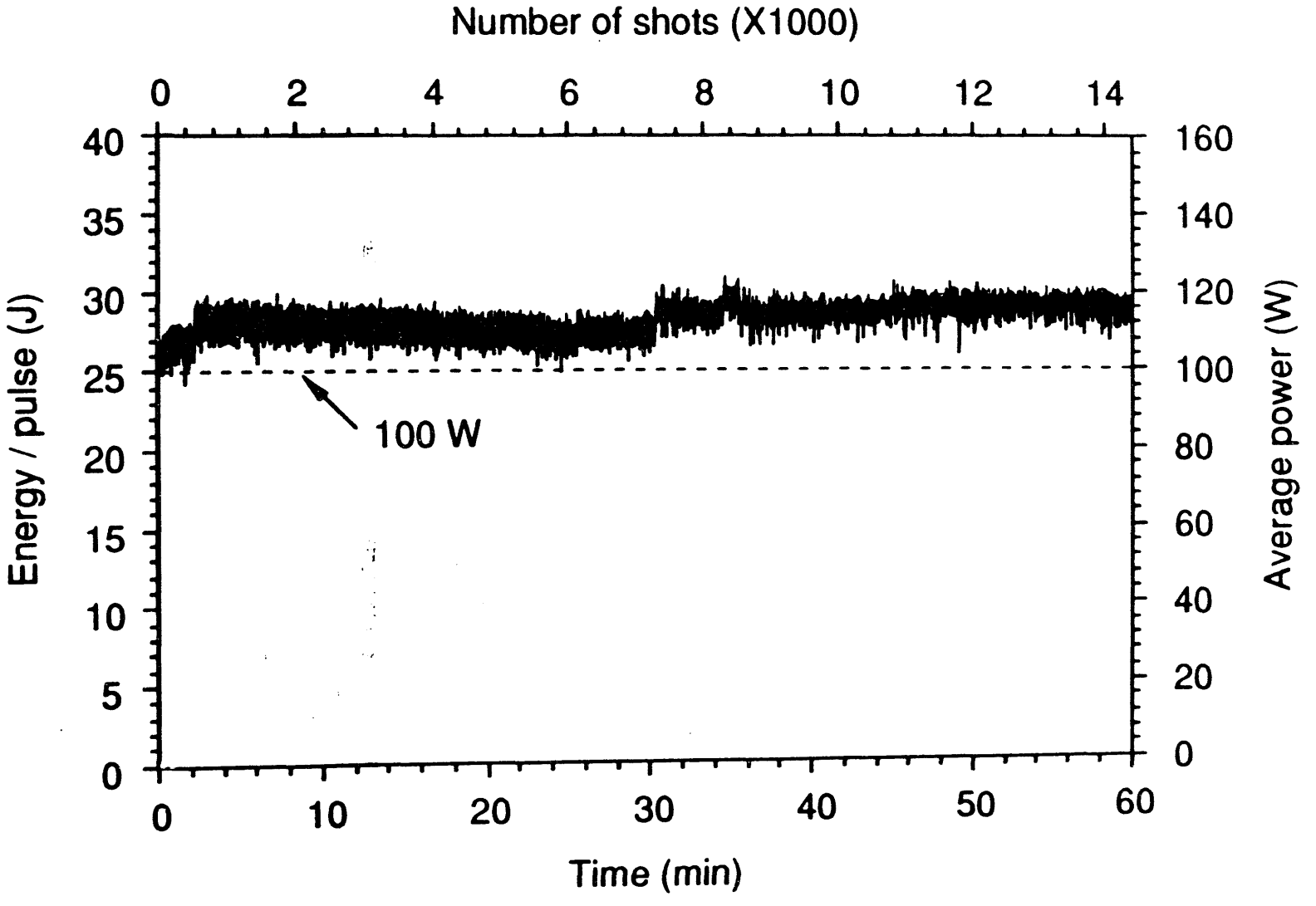
Number of shots (X1000)
0
2
4
6
8
10
12
14
Energy / pulse (J)
40
35
30
25
20
15
10
5
0
100 W
Average power (W)
160
140
120
100
80
60
40
20
0
0
10
20
30
40
50
60
Time (min)

Fig. 6

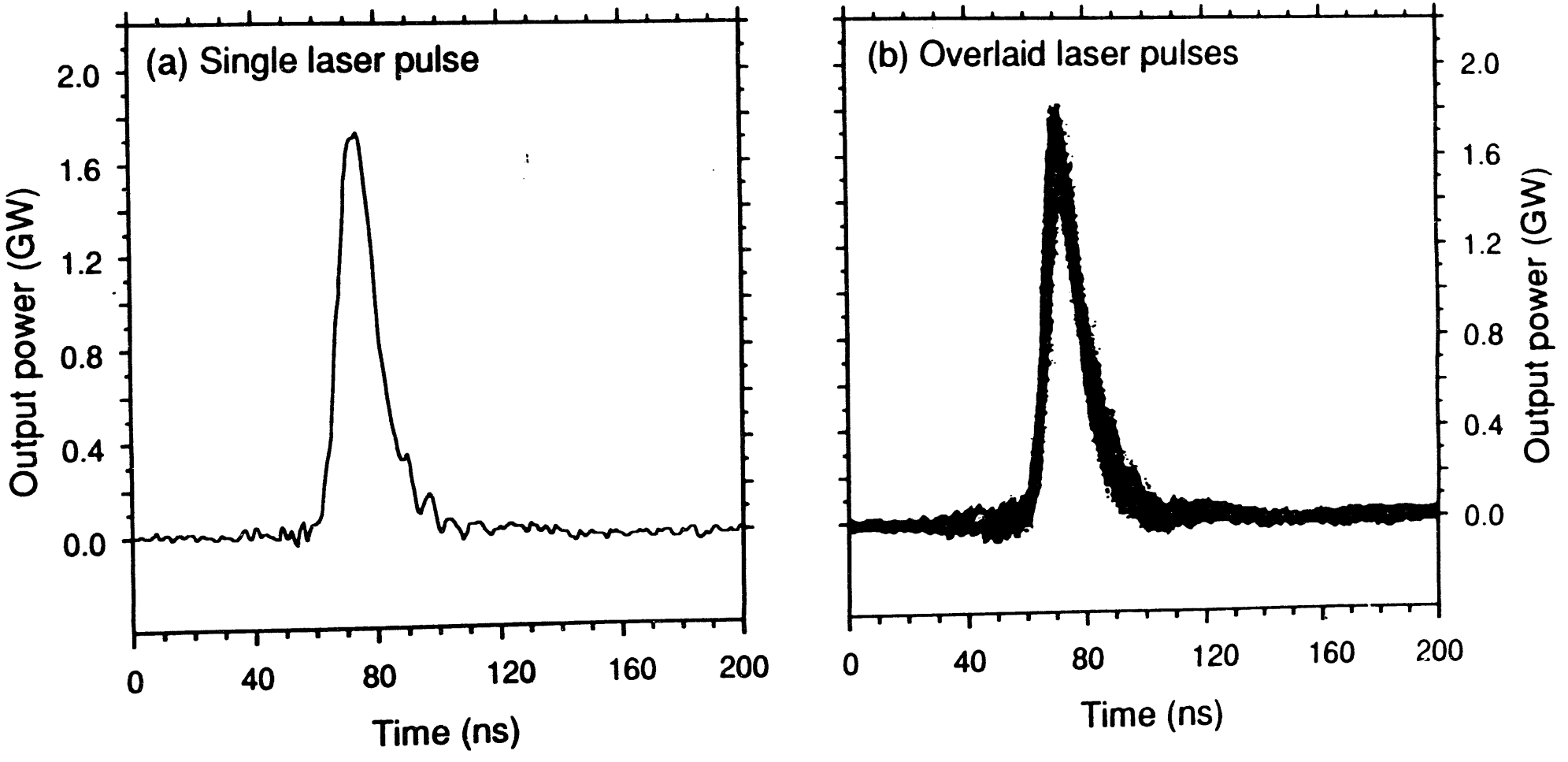
(a) Single laser pulse
(b) Overlaid laser pulses
Output power (GW)
2.0
1.6
1.2
0.8
0.4
0.0
0
40
80
120
160
200
Time (ns)

Fig. 7

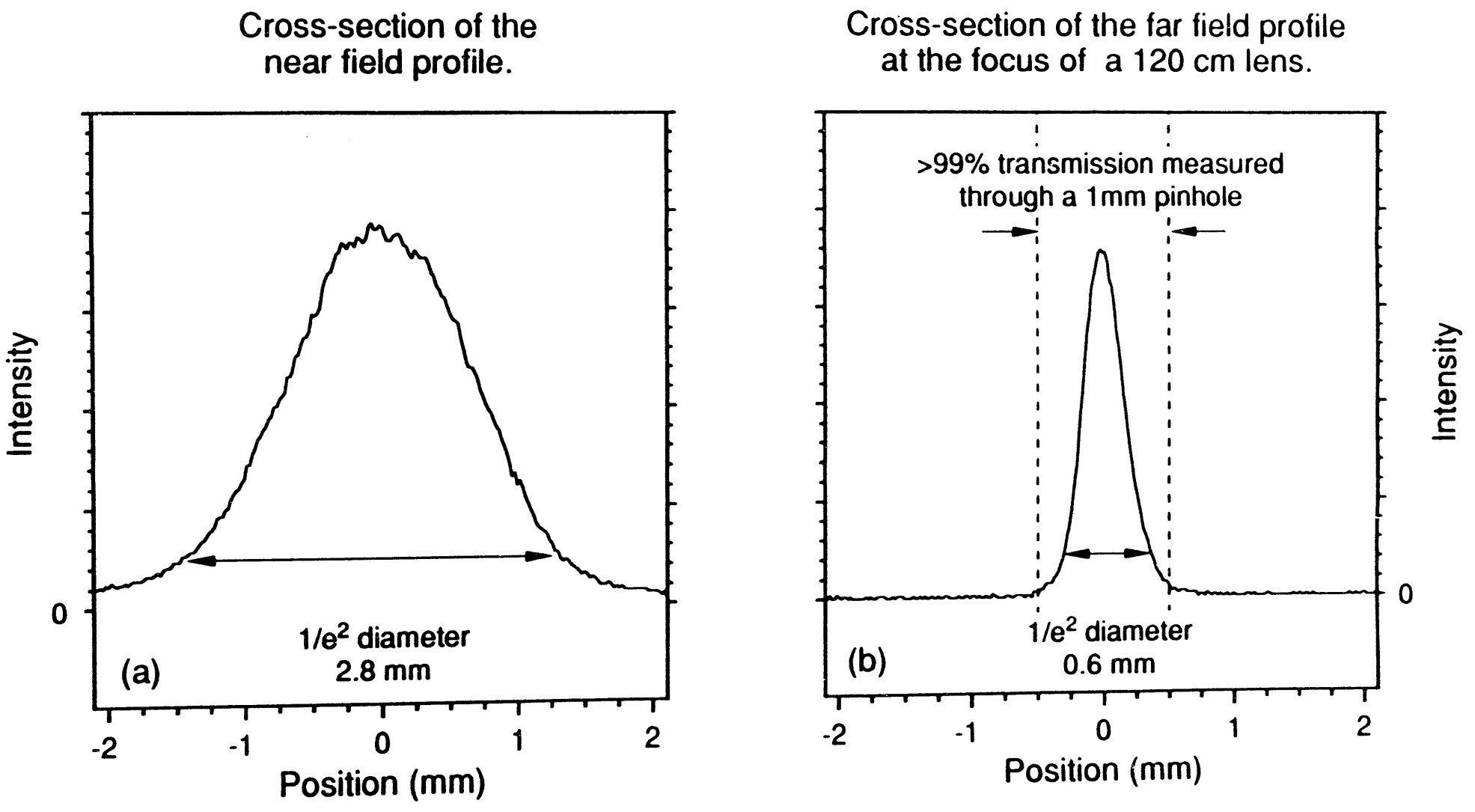
Cross-section of the
near field profile.
Intensity
0
1/e² diameter
2.8 mm
(a)
-2
-1
0
1
2
Position (mm)
Cross-section of the far field profile
at the focus of a 120 cm lens.
>99% transmission measured
through a 1mm pinhole
1/e² diameter
0.6 mm
(b)
Intensity
0
-2
-1
0
1
2
Position (mm)

Fig. 8

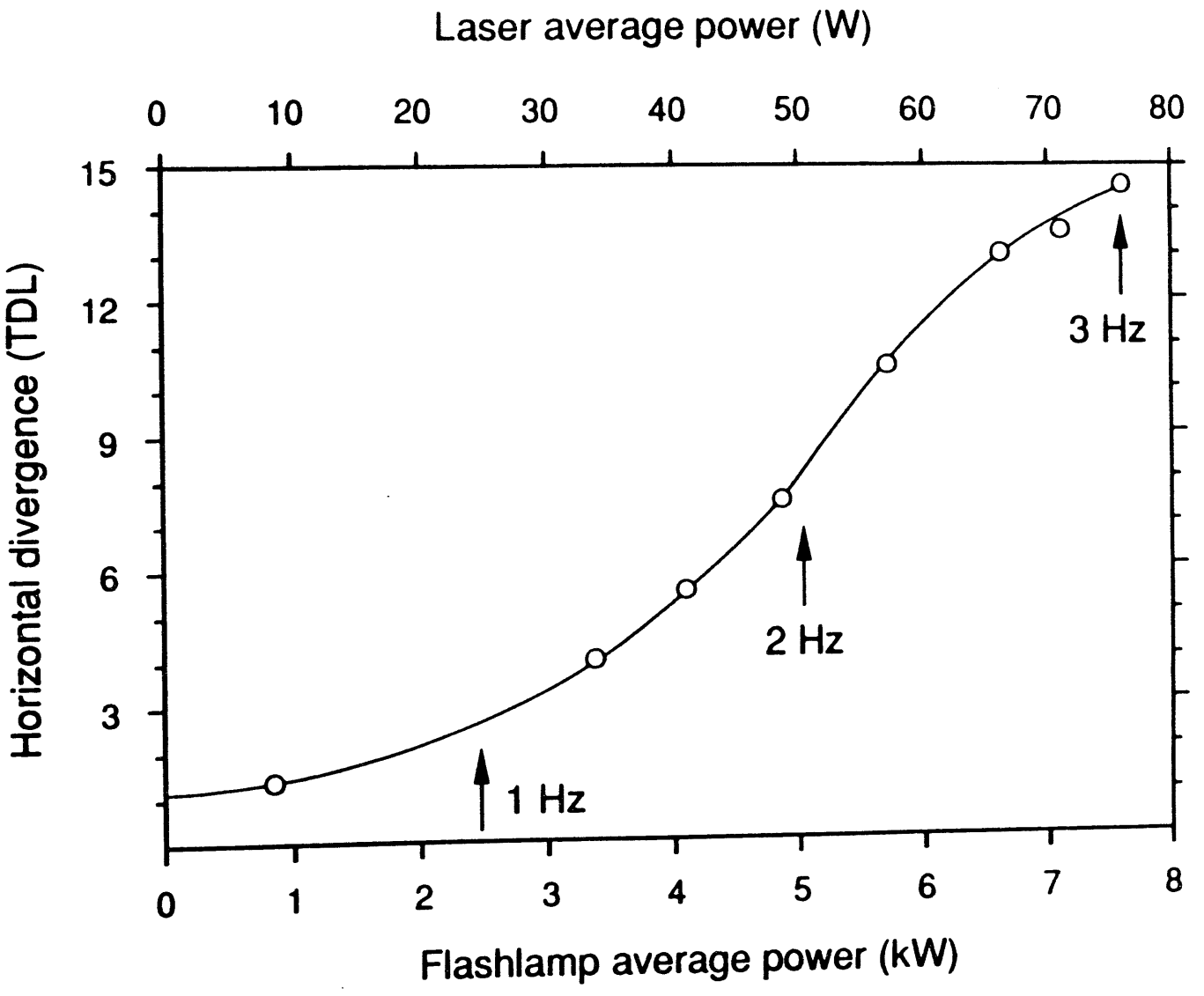
Laser average power (W)
0
10
20
30
40
50
60
70
80
15
12
9
6
3
Horizontal divergence (TDL)
1 Hz
2 Hz
3 Hz
0
1
2
3
4
5
6
7
8
Flashlamp average power (kW)

Fig. 9

(a) Without SBS phase conjugation

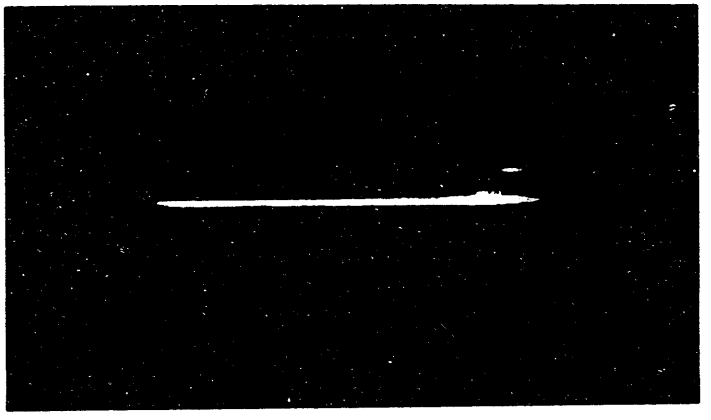

(b) With SBS phase conjugation

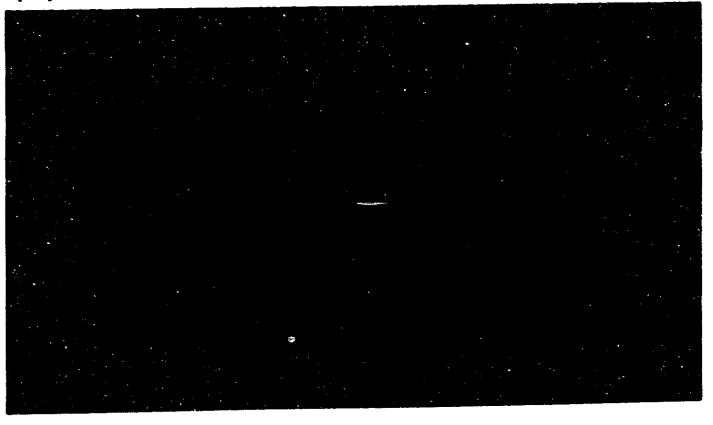

(c) Output divergence for 25 J, 3 Hz operation

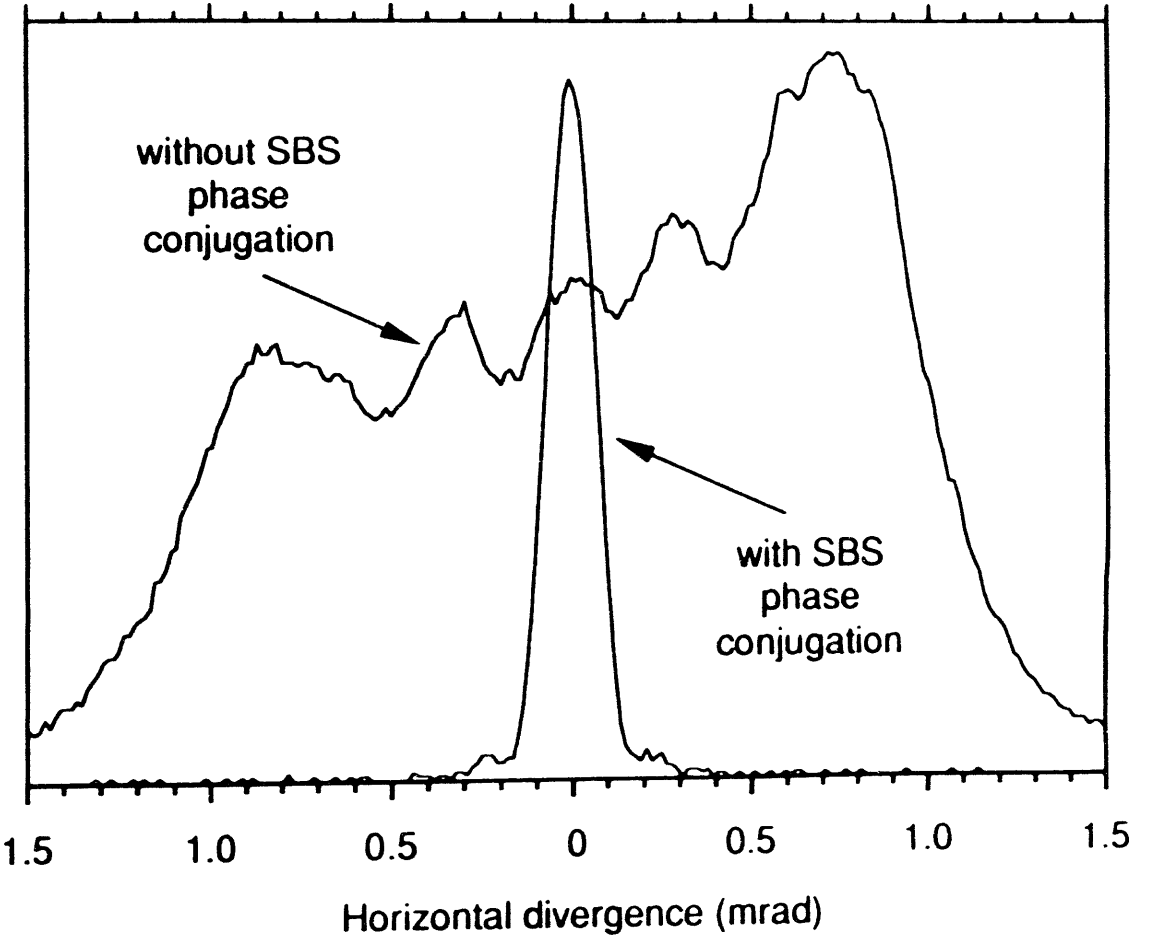

Fig. 10

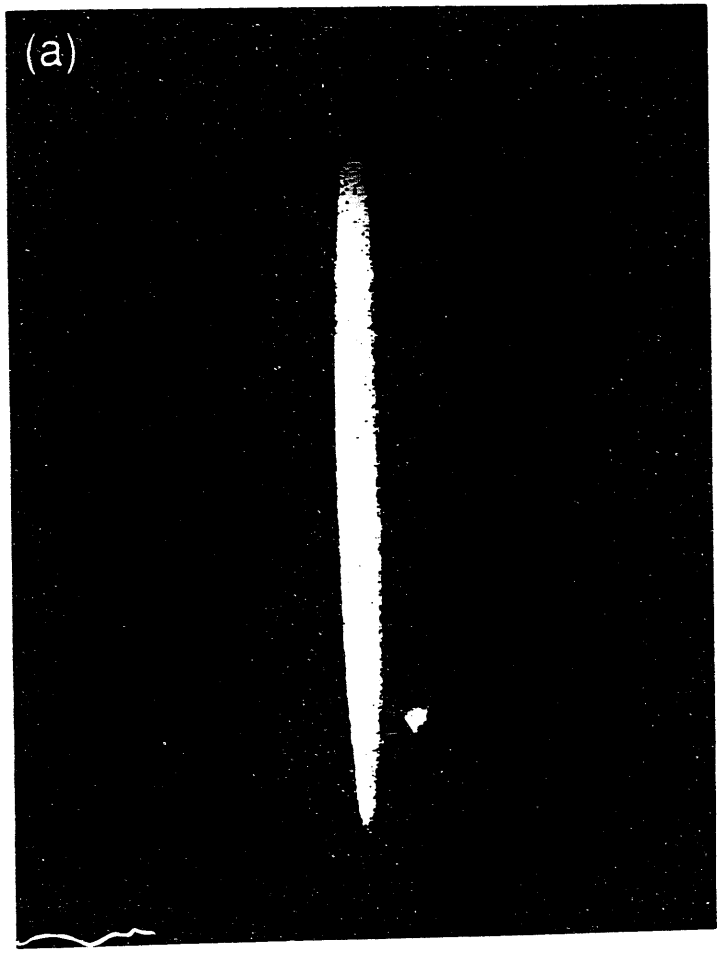
(a)

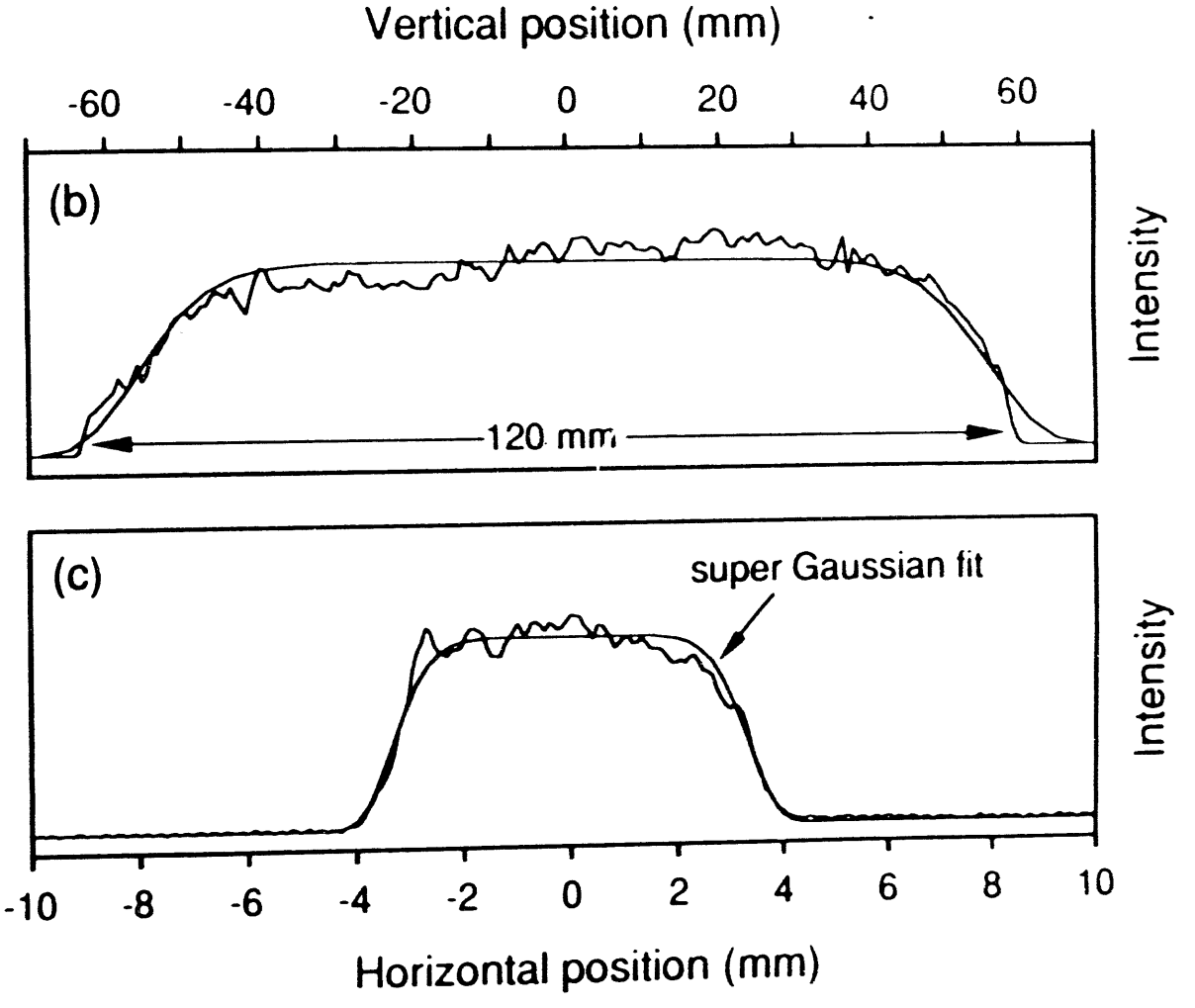
Vertical position (mm)
-60
-40
-20
0
20
40
60
(b)
120 mm
Intensity
(c)
super Gaussian fit
Intensity
-10
-8
-6
-4
-2
0
2
4
6
8
10
Horizontal position (mm)

Fig. 11

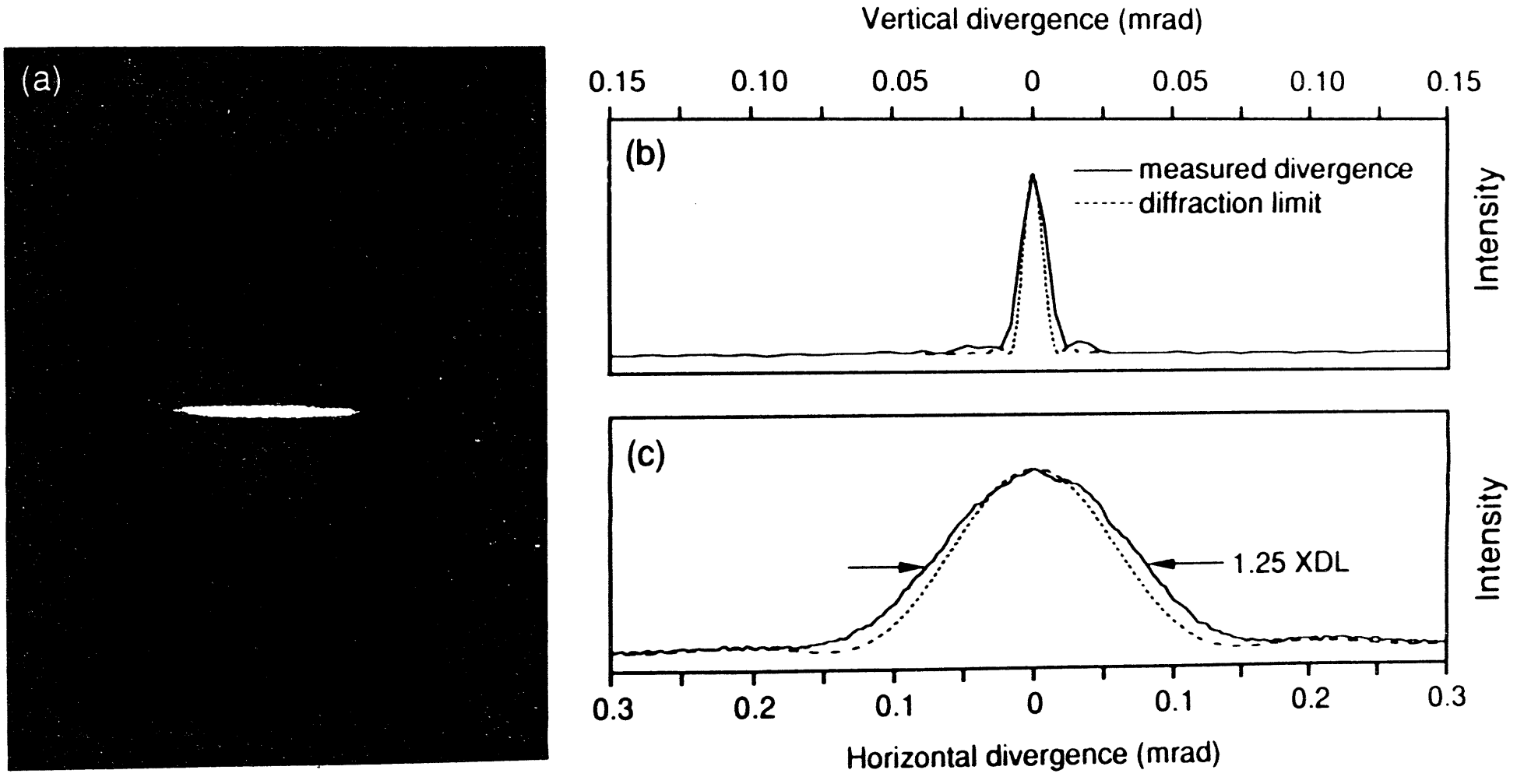
(a)
Vertical divergence (mrad)
0.15
0.10
0.05
0
0.05
0.10
0.15
(b)
measured divergence
diffraction limit
Intensity
(c)
1.25 XDL
Intensity
0.3
0.2
0.1
0
0.1
0.2
0.3
Horizontal divergence (mrad)

Fig. 12

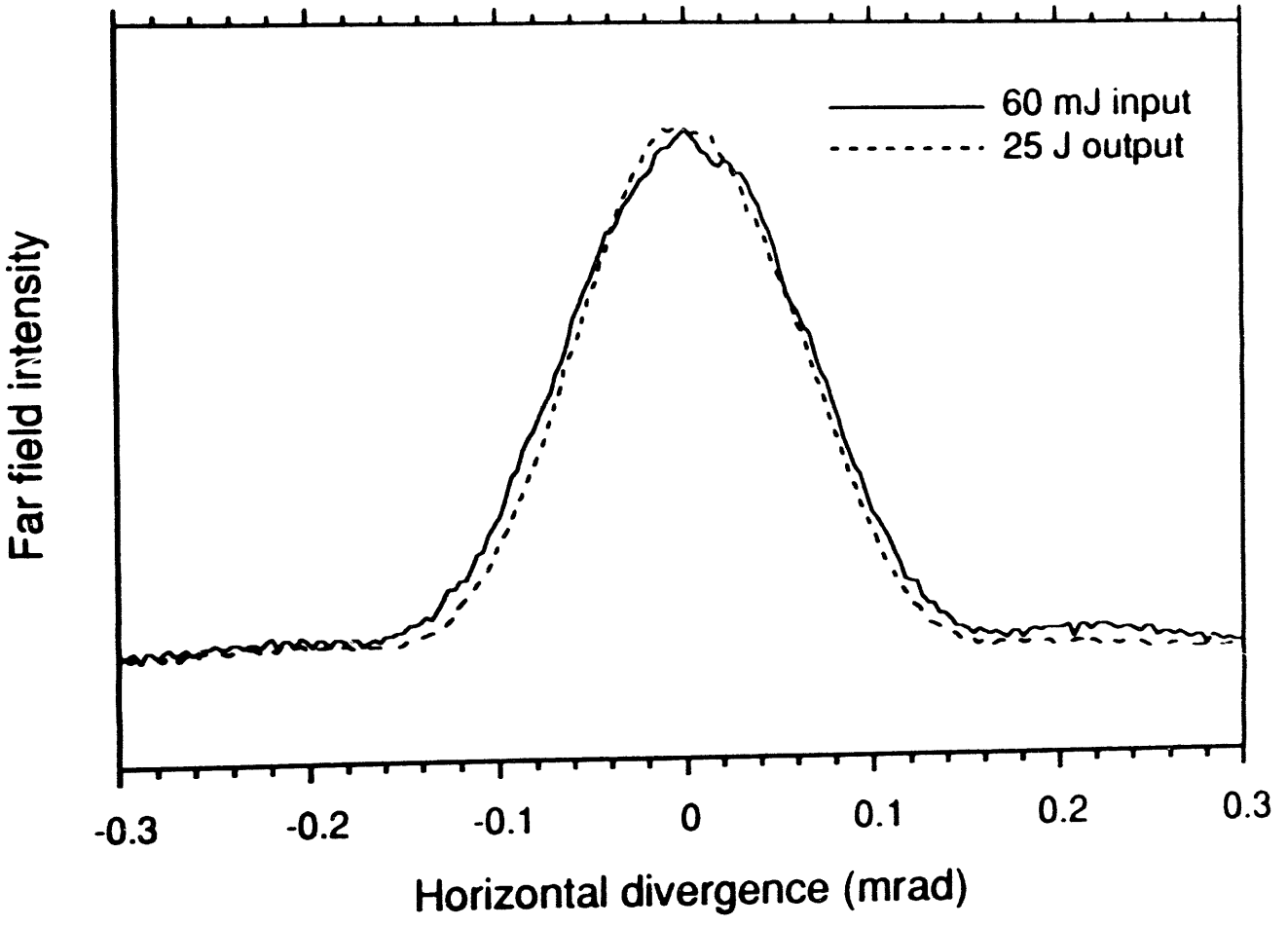
60 mJ input
25 J output
Far field intensity
-0.3
-0.2
-0.1
0
0.1
0.2
0.3
Horizontal divergence (mrad)

Fig. 13

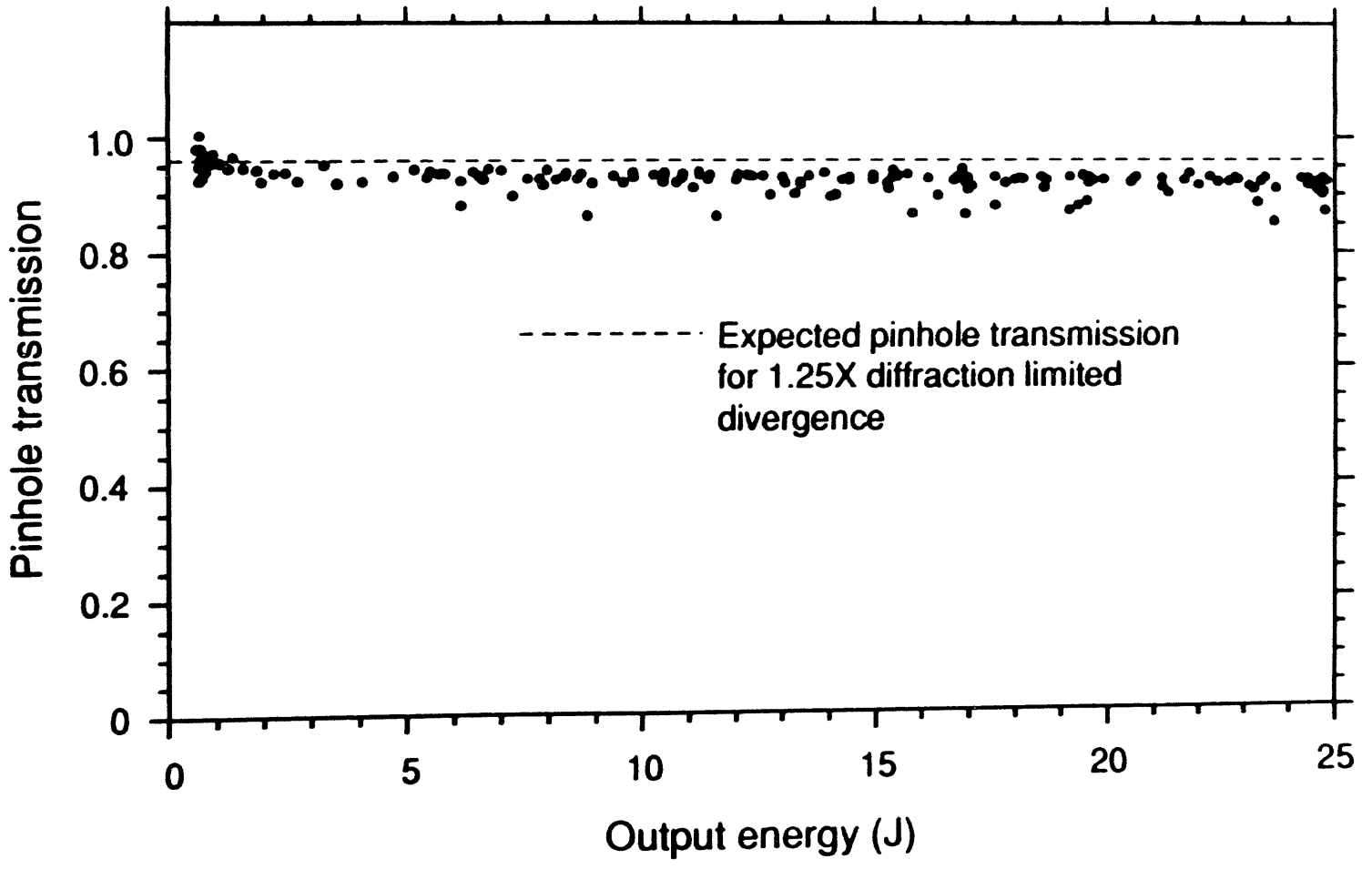
Pinhole transmission
1.0
0.8
0.6
0.4
0.2
0
0
5
10
15
20
25
Output energy (J)
Expected pinhole transmission
for 1.25X diffraction limited
divergence

Fig. 14

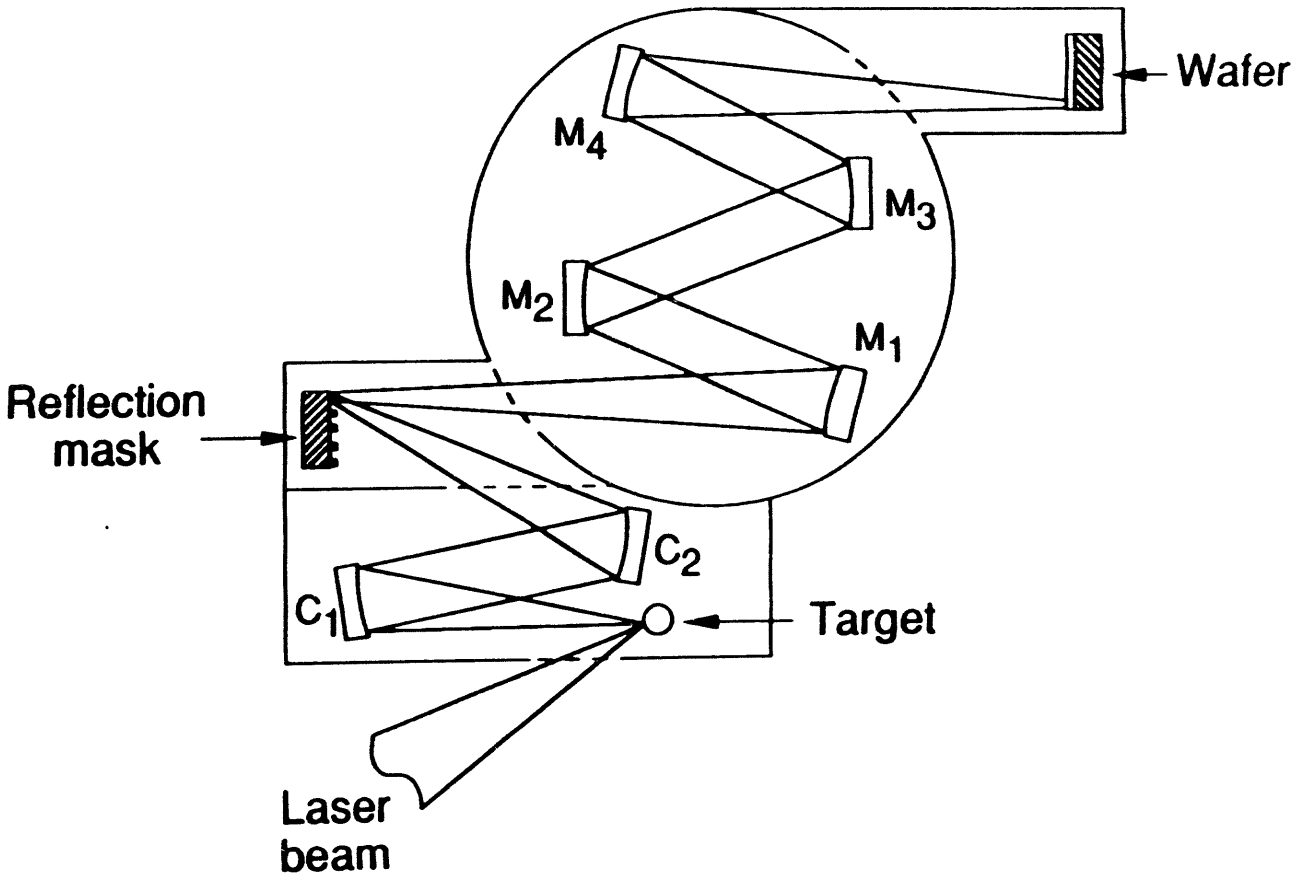

Fig. 15

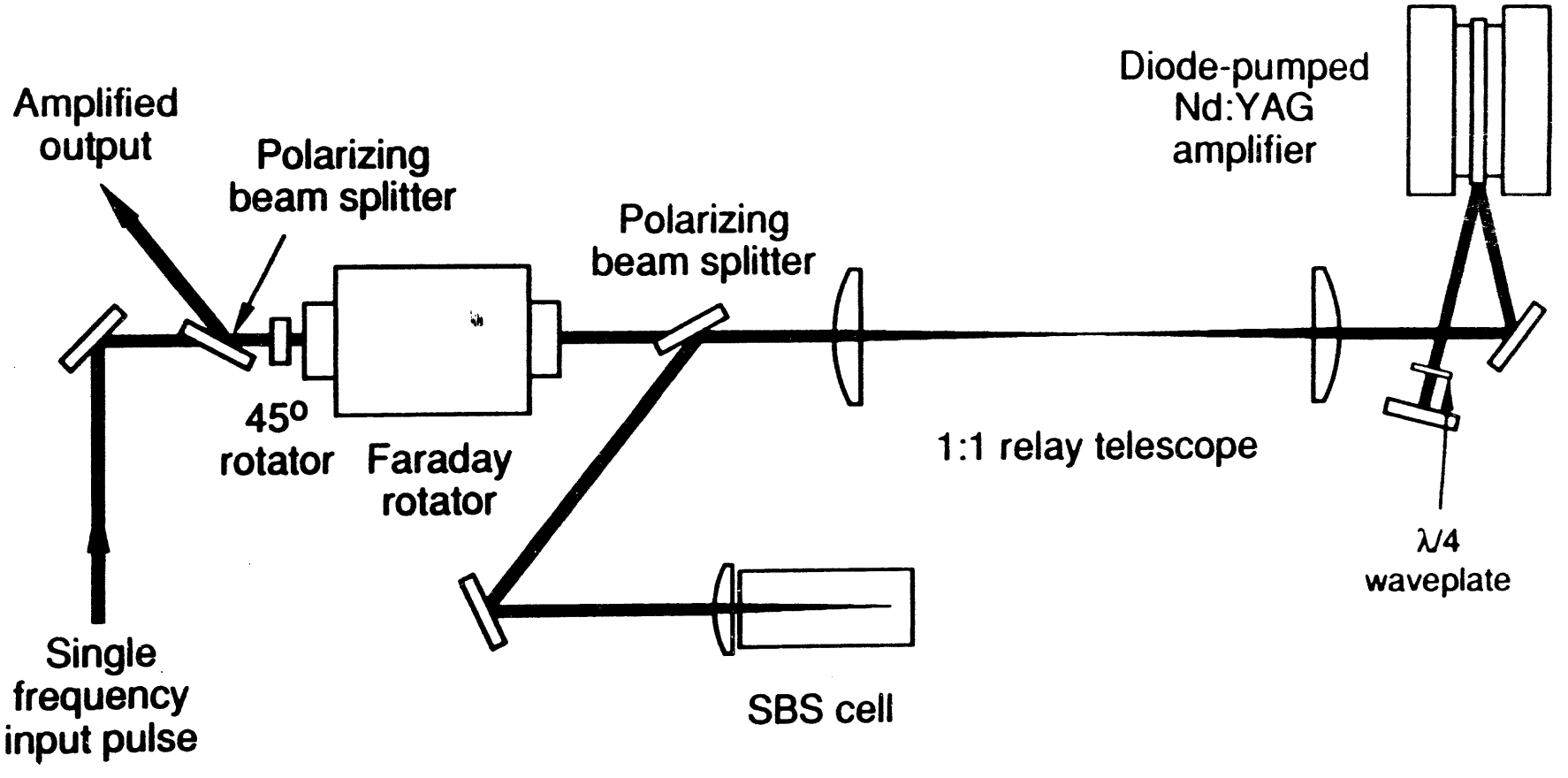
Amplified output
Polarizing beam splitter
45° rotator
Faraday rotator
Polarizing beam splitter
Diode-pumped Nd:YAG amplifier
1:1 relay telescope
λ/4 waveplate
Single frequency input pulse
SBS cell

Fig. 16

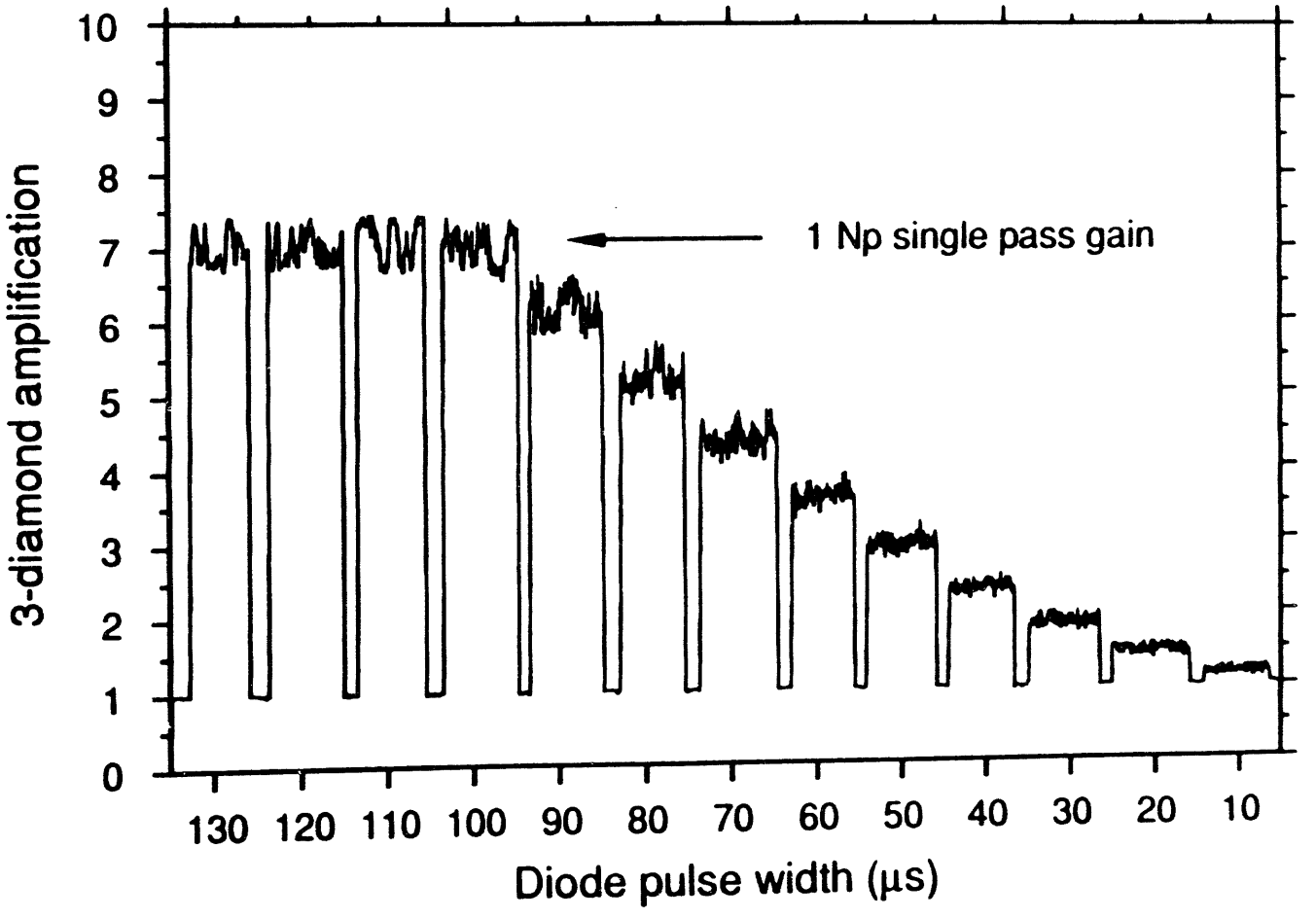
3-diamond amplification
10
9
8
7
6
5
4
3
2
1
0
1 Np single pass gain
130 120 110 100 90 80 70 60 50 40 30 20 10
Diode pulse width (μs)

Fig. 17

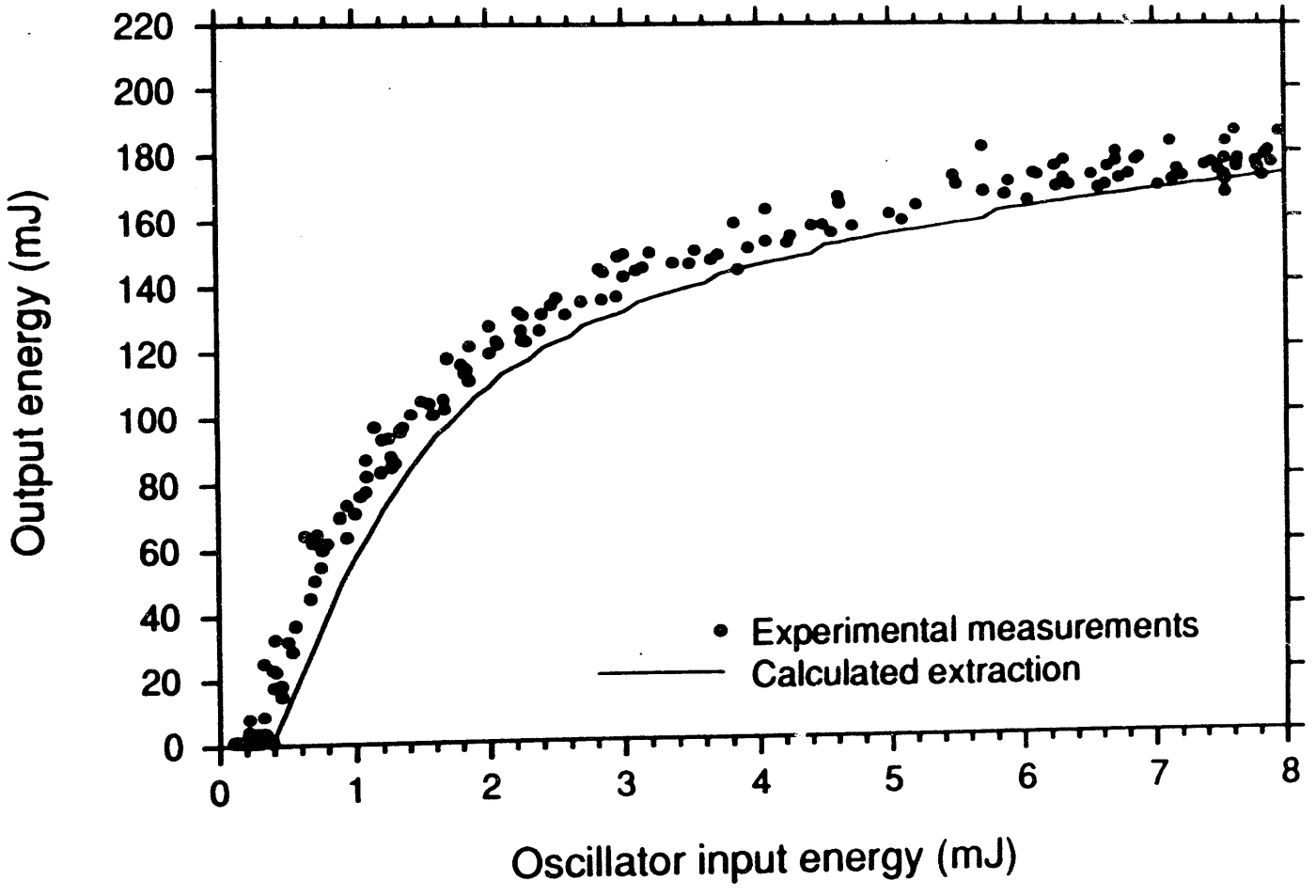
Output energy (mJ)
220
200
180
160
140
120
100
80
60
40
20
0
0
1
2
3
4
5
6
7
8
Oscillator input energy (mJ)
Experimental measurements
Calculated extraction

Fig. 18

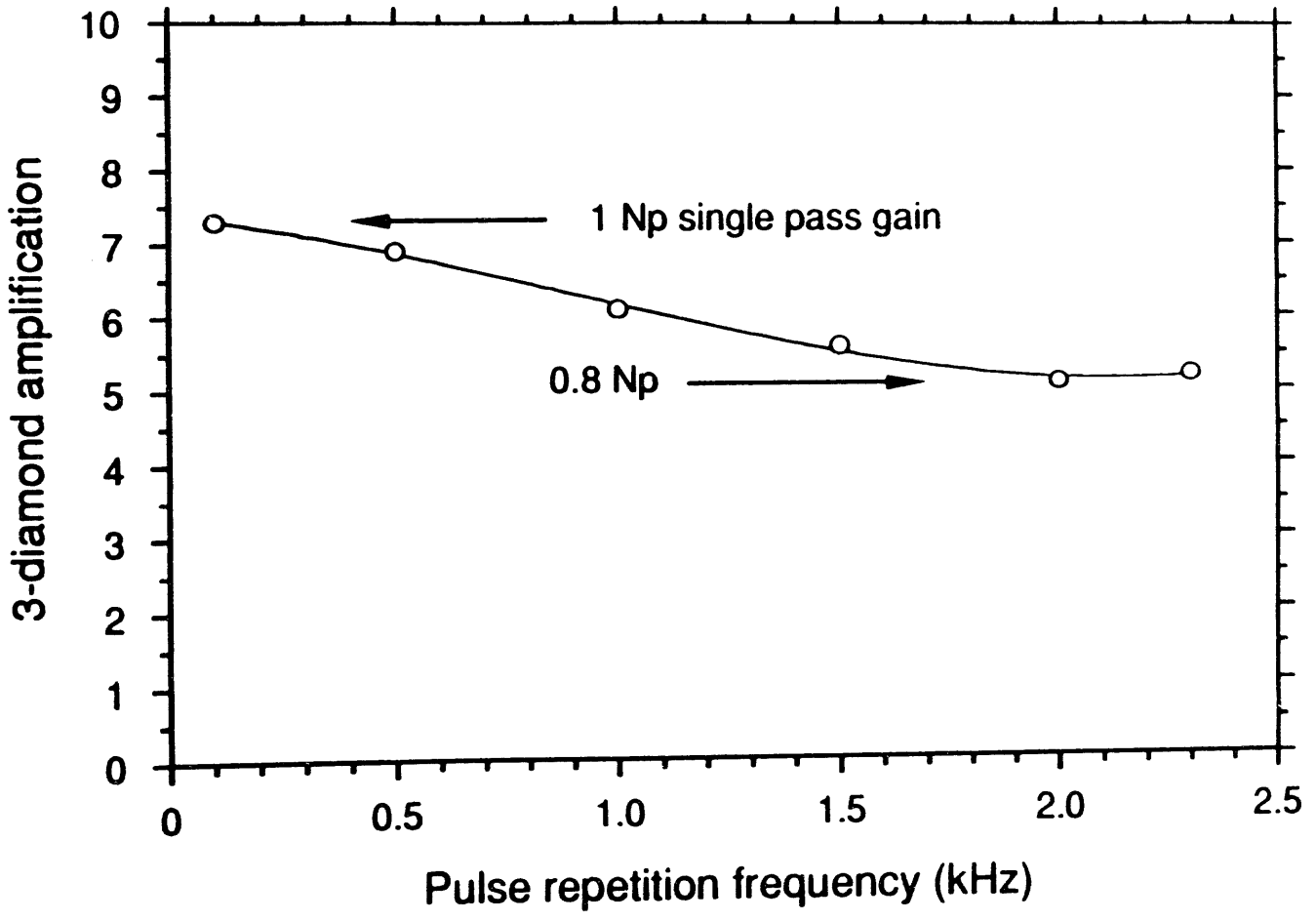
3-diamond amplification
10
9
8
7
6
5
4
3
2
1
0
1 Np single pass gain
0.8 Np
0
0.5
1.0
1.5
2.0
2.5
Pulse repetition frequency (kHz)

Fig. 19

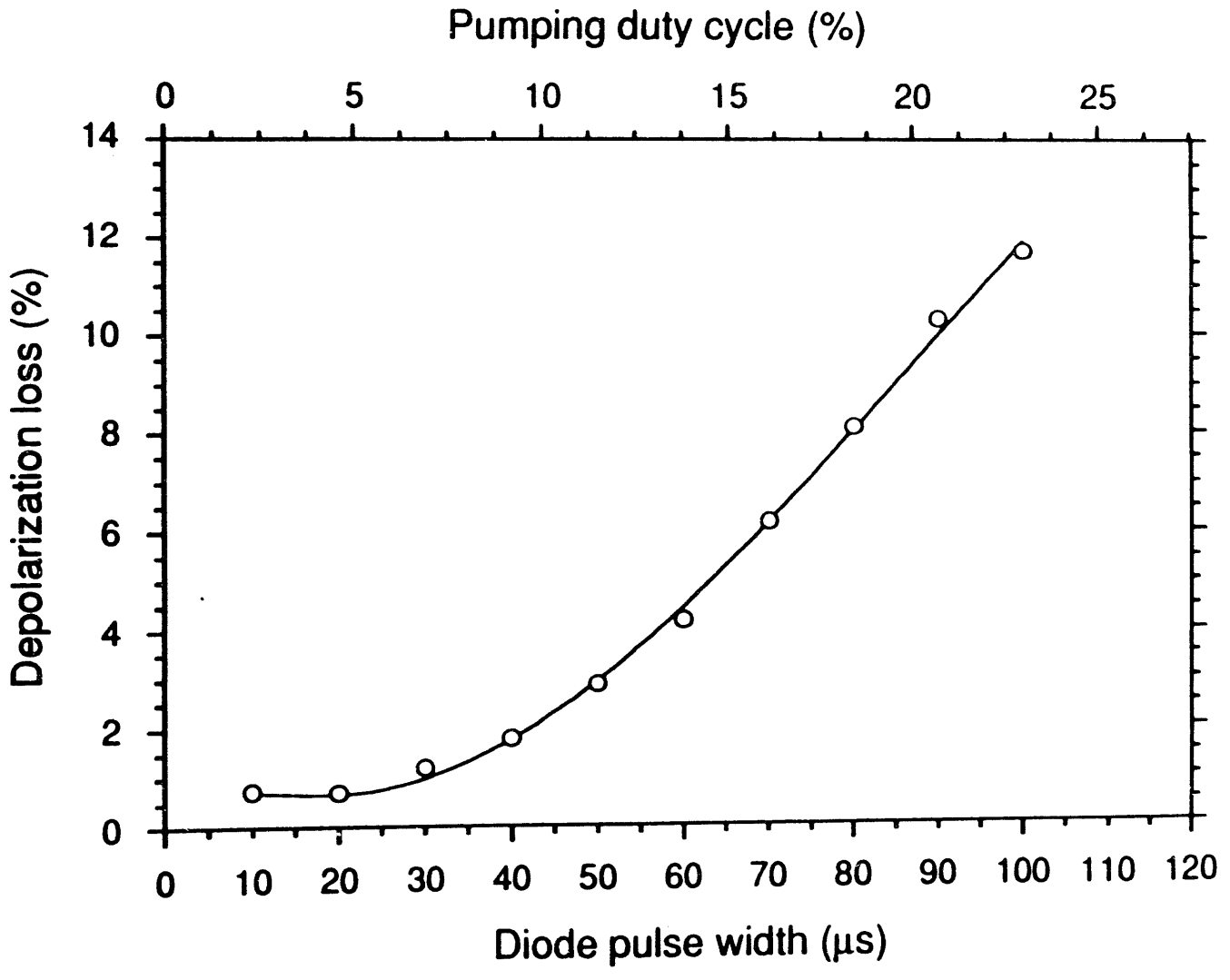
Pumping duty cycle (%)
0
5
10
15
20
25
Depolarization loss (%)
14
12
10
8
6
4
2
0
0
10
20
30
40
50
60
70
80
90
100
110
120
Diode pulse width (μs)

Fig. 20

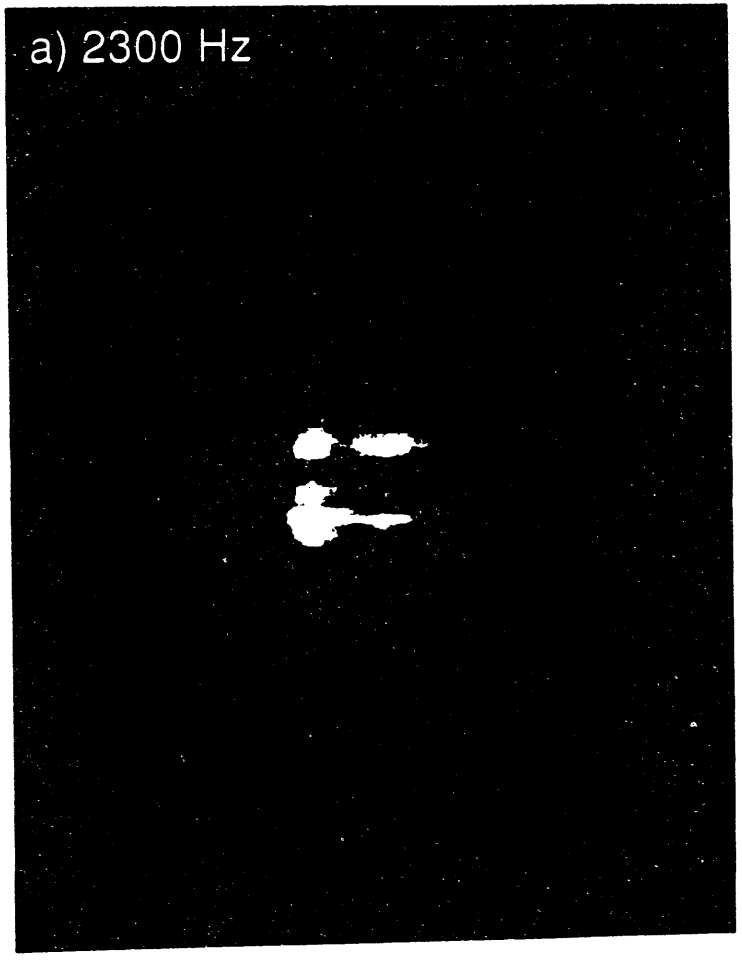
a) 2300 Hz

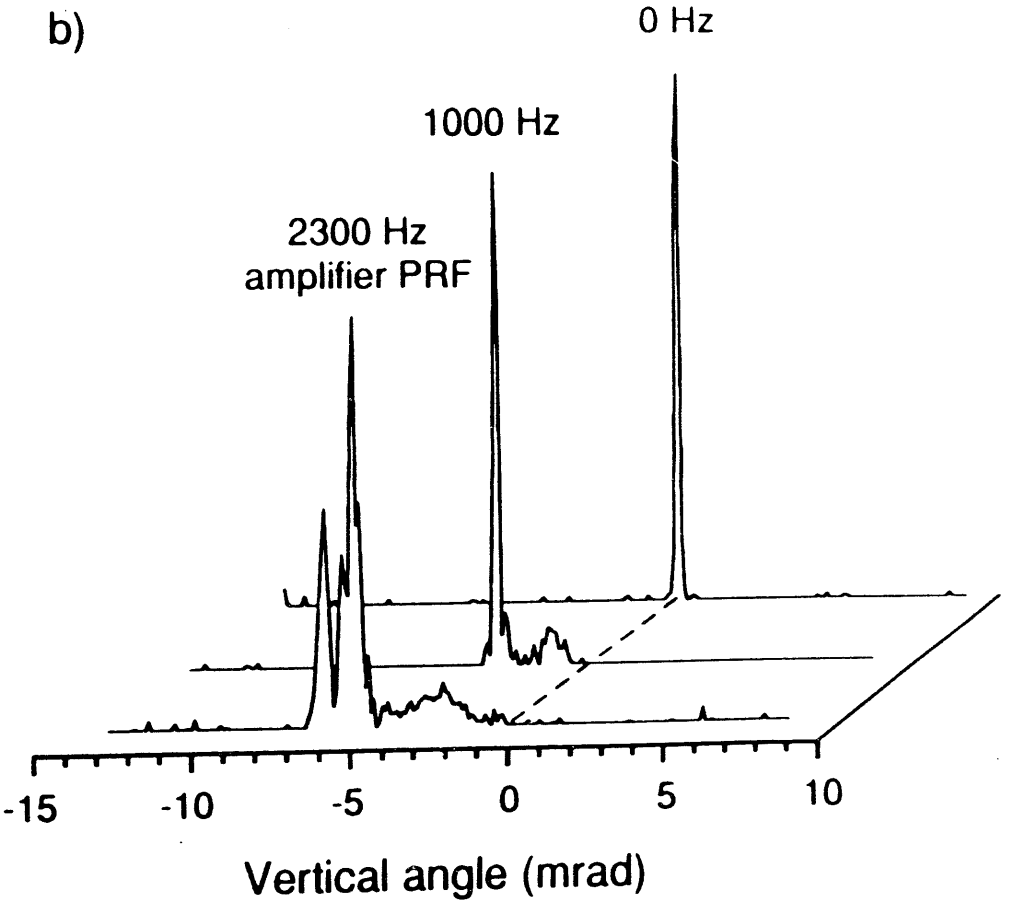
b)
0 Hz
1000 Hz
2300 Hz
amplifier PRF
-15
-10
-5
0
5
10
Vertical angle (mrad)

Fig. 21

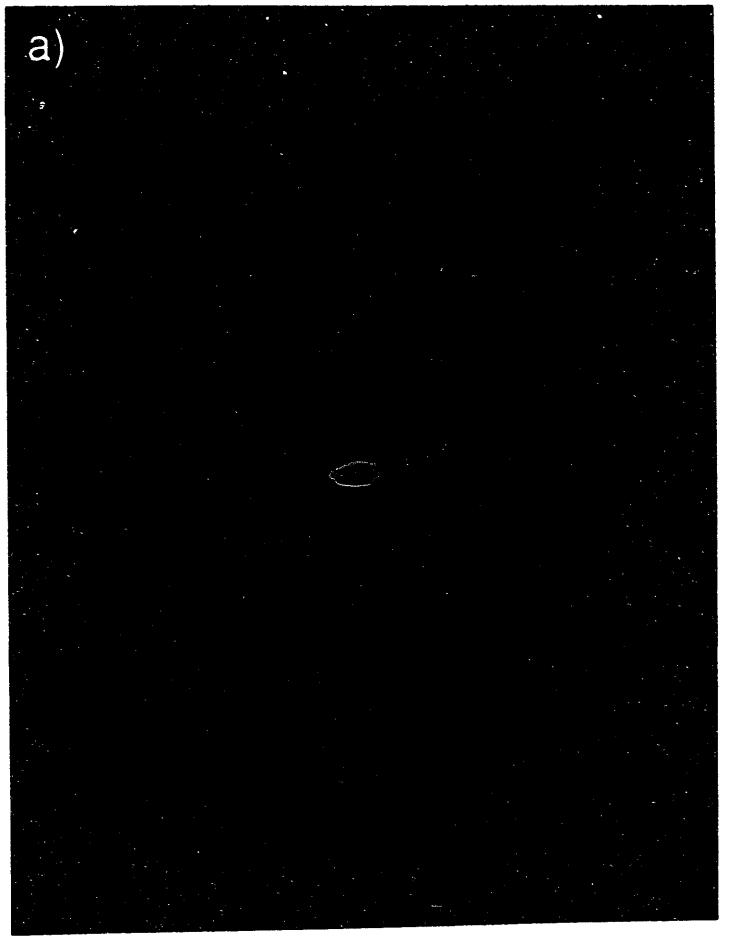
a)

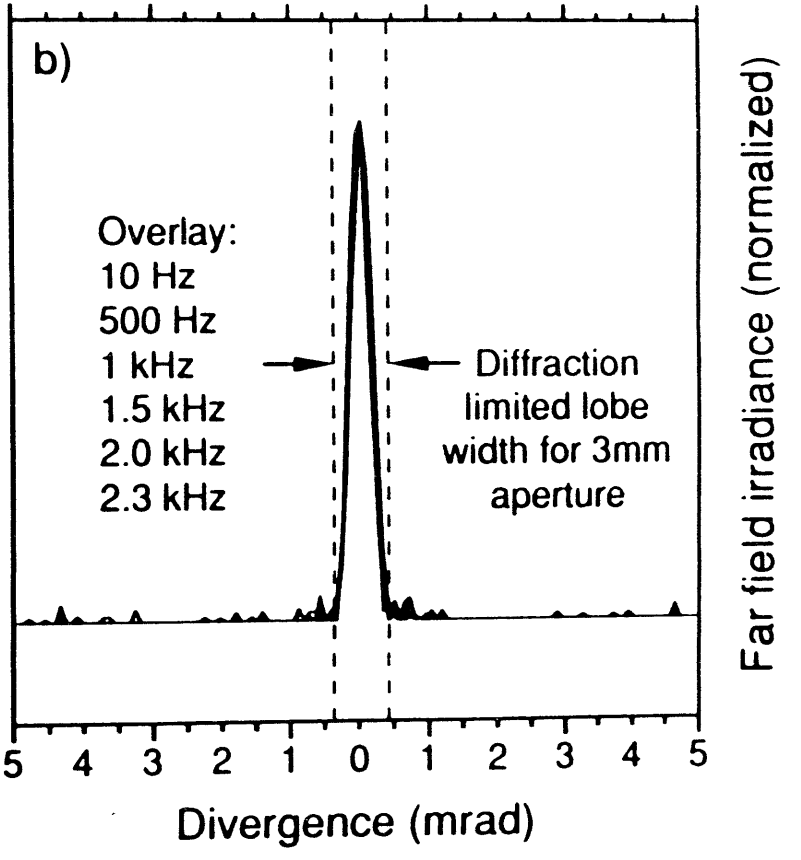
b)
Overlay:
10 Hz
500 Hz
1 kHz
1.5 kHz
2.0 kHz
2.3 kHz
Diffraction limited lobe width for 3mm aperture
5 4 3 2 1 0 1 2 3 4 5
Divergence (mrad)
Far field irradiance (normalized)

Fig. 22

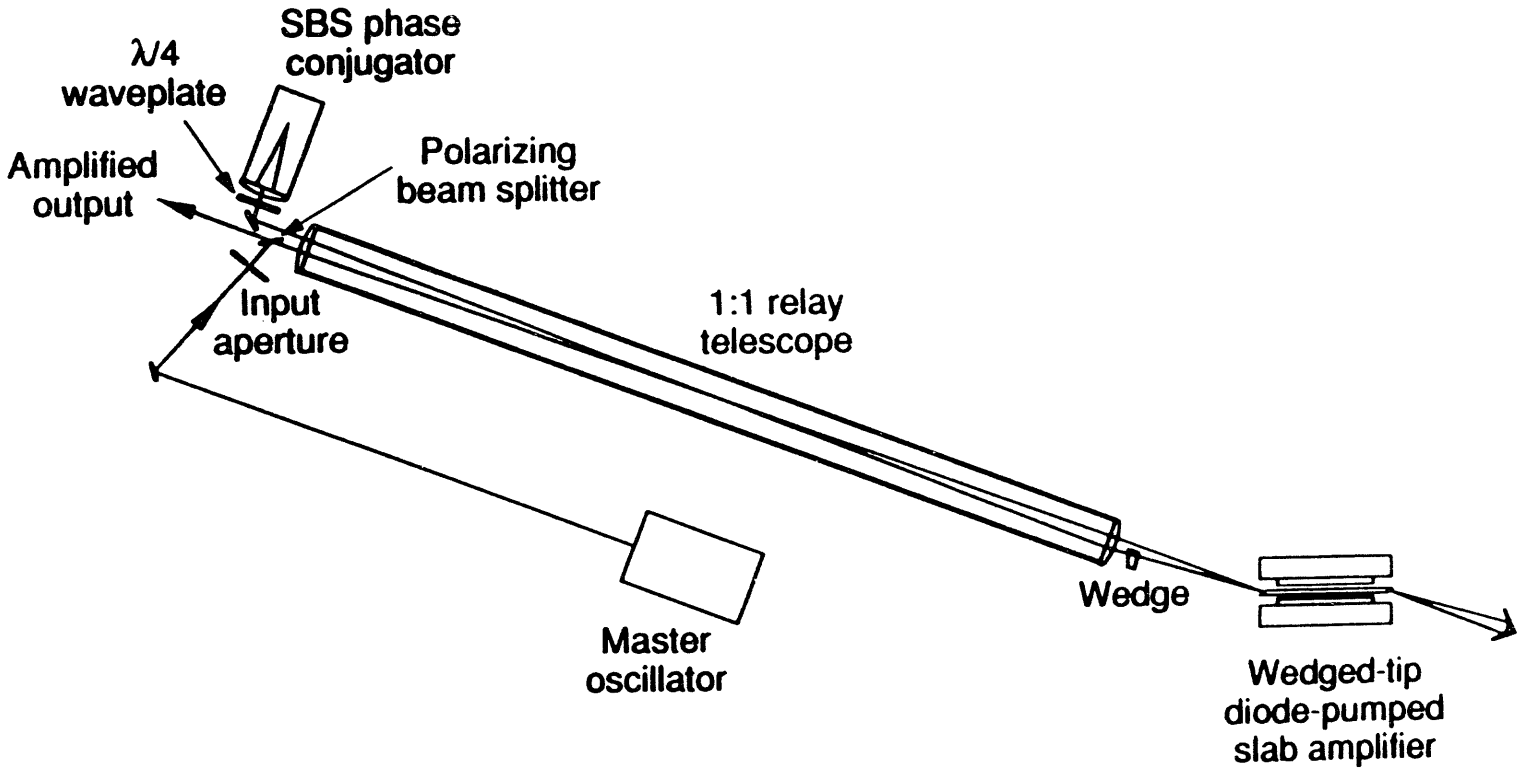
SBS phase
conjugator
λ/4
waveplate
Amplified
output
Polarizing
beam splitter
Input
aperture
1:1 relay
telescope
Master
oscillator
Wedge
Wedged-tip
diode-pumped
slab amplifier

Fig. 23

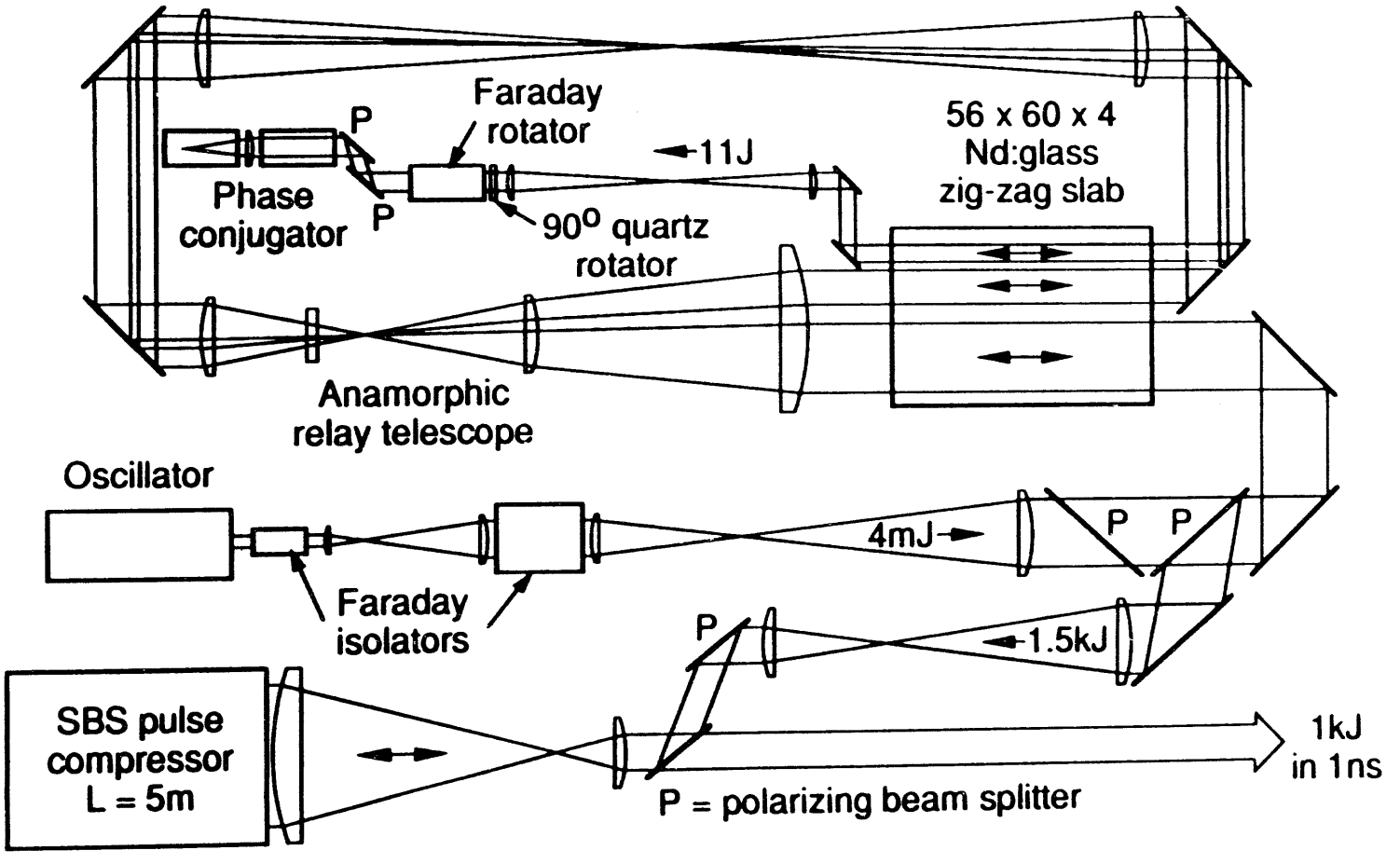
Faraday
rotator
P
P
Phase
conjugator
11J
90° quartz
rotator
56 x 60 x 4
Nd:glass
zig-zag slab
Anamorphic
relay telescope
Oscillator
4mJ
P
P
Faraday
isolators
P
1.5kJ
SBS pulse
compressor
L = 5m
1kJ
in 1ns
P = polarizing beam splitter

Fig. 24

DATE
FILMED
9/1/94

END